



Universiteit
Leiden
The Netherlands

Control of early plant development by light quality

Spaninks, K.

Citation

Spaninks, K. (2023, May 10). *Control of early plant development by light quality*. Retrieved from <https://hdl.handle.net/1887/3618264>

Version: Publisher's Version

License: [Licence agreement concerning inclusion of doctoral thesis in the Institutional Repository of the University of Leiden](#)

Downloaded from: <https://hdl.handle.net/1887/3618264>

Note: To cite this publication please use the final published version (if applicable).

Chapter 5

Light quality regulates flowering through the photoperiodic and age pathways.

Kiki Spaninks¹ and Remko Offringa¹

¹Plant Developmental Genetics, Institute of Biology Leiden,
Leiden University, Sylviusweg 72, 2333 BE, Leiden, Netherlands.



Abstract

For leafy horticultural crops, such as lettuce and cabbage, delayed flowering is essential for quality crop production, whereas breeders require early flowering to speed up seed production cycles and breeding programs. Environmental cues such as temperature, photoperiod, or light quality have been used to control flowering time and especially the currently available LED technology allows accurate spectral quality control. Although previous LED studies have shown that many phenotypic traits of different plant species can be modulated by light quality, most of their underlying molecular mechanisms remain unknown, which makes their application on other crop species unpredictable. Here, we combined genetic studies of flowering pathways in the long-day model dicot *Arabidopsis thaliana* (*Arabidopsis*), with physiological experiments in long-day and day-neutral *Lactuca sativa* (lettuce) and *Solanum lycopersicum* (tomato) plants. Using LEDs, we confirmed that blue light must be present in the spectrum to activate the photoperiodic pathway to promote flowering in the long-day plant species. In addition, we identified a new flowering-inhibiting role for red light in the spectrum that represses the age pathway in long-day and (some) day-neutral plant species. We identified PHYB as an inhibitor of plant ageing through its activation of *microRNA156*, which represses the flower-promoting SQUAMOSA-PROMOTER BINDING PROTEIN-LIKE (SPL) transcription factors. Our findings identify a molecular pathway that integrates plant ageing and light quality in *Arabidopsis*, and that may be conserved in important crop species.



Keywords: Flowering, Photoperiod, Ageing, PHYB, miR156, SPLs, GIGANTEA

Introduction

Various environmental factors, such as light, temperature and stress determine the timing of the floral transition, and thus offer potential control over the plant life cycle (Thomas, 2006; Cho et al., 2017). In horticulture, environmental control of flowering would be useful to speed up production cycles for important crops such as tomato (*Solanum lycopersicum*). Moreover, plant breeding programs would greatly benefit from floral induction in response to changing environmental cues, especially in plants species that have been bred towards late flowering, such as lettuce (*Lactuca sativa*). Because of their possibility for spectral quality control, LEDs may be used to steer plant development towards early or late flowering (Morrow, 2008; SharathKumar et al., 2020). To achieve this, we must elucidate the molecular mechanisms that underly the flowering response to light quality and explore how these mechanisms are conserved in different plant species. The effect of light quality on flowering has been extensively studied with the use of photoreceptor mutants in the genetic model dicot *Arabidopsis thaliana* (Arabidopsis). In Arabidopsis, diurnal accumulation of the blue light photoreceptor *FLAVIN-BINDING, KELCH REPEAT, F-BOX 1* (FKF1) and the nuclear protein *GIGANTEA* (GI) coincides during long day photoperiods. FKF1, through interaction with its two other blue light-activated family members *ZEITLUPE* (ZTL) and *LOV KELCH PROTEIN 2* (LKP2), associates with GI to inhibit



Chapter 5: Light quality regulates flowering

expression of *CYCLING DOF FACTORs* (CDFs) that repress expression of *CONSTANS* (*CO*) (Sawa et al., 2007; Fornara et al., 2009). In addition, *CO* transcription is promoted by the blue light receptor cryptochrome 2 (*CRY2*) and the FR-activated phytochrome A (*PHYA*) (Valverde et al., 2004; Liu et al., 2008). As a result, *CO* levels rise and peak during the late afternoon, which subsequently results in elevated expression of *FLOWERING LOCUS T* (*FT*) at the end of the day (Samach et al., 2000). Finally, this *FT* peak promotes flowering through activation of floral meristem identity genes such as *APETALA 1* (*API*) and *FRUITFULL* (*FUL*) (Abe et al., 2005; Wigge et al., 2005). In contrast to blue and FR light-inducible photoreceptors, the red light-activated phytochrome B (*PHYB*) inhibits flowering through targeted degradation of *CO* (Valverde et al., 2004; Lazaro et al., 2015), and possibly through inhibition of *GI*, an interaction opposite to *PHYB* function during hypocotyl elongation (Huq et al., 2000). Although photoreceptor studies in *Arabidopsis* have contributed greatly to the understanding of photoperiodic flowering, light quality studies using LEDs, where the activity of all photoreceptors are influenced simultaneously, remain limited. Moreover, light quality responses should be investigated in different long-day (LD), short-day (SD) and day-neutral (DN) species. As a main integrator of circadian clock components and light signalling, homologs of *CO* have been identified in both LD and SD species (Robert et al., 1998; Yano et al., 2000; Campoli et al., 2012; Yang et al., 2014), suggesting that the photoperiodic pathway is the main light-regulated flowering pathway. However, this would also suggest that flowering of DN species is either indifferent to light quality, which is in line with our previous study in tomato (**chapter 3**), or that light quality regulates flowering through other pathways as well. In addition to the photoperiodic pathway, the



floral transition depends on four other pathways: vernalization, gibberellic acid (GA), autonomous regulation, and plant ageing (Teotia and Tang, 2015). Although studies concerning the effect of light quality on these other pathways remain limited, there is some evidence for light-regulated flowering that is photoperiod-independent. For example, *Arabidopsis phyB* mutant plants show early flowering compared to wild type, both under LD and SD photoperiods (Reed et al., 1993), thus indicating an additional photoperiod-independent role for PHYB in flowering. Moreover, diurnal expression levels of *CO* and *FT* are similar in *phyB* and wild-type plants, suggesting once more that PHYB may act independent of photoperiod. Although PHYB modulates responsiveness to GA during hypocotyl elongation, PHYB-dependent flowering has been shown to be GA-independent (Blázquez and Weigel, 1999). However, two recent shade avoidance studies show that downstream signalling targets of PHYA, and possibly of PHYB, modulate plant ageing. Under low R:FR ratios, *microRNA156* (*miR156*) is repressed, which alleviates its inhibitory effect on the expression of SQUAMOSA-PROMOTER BINDING PROTEIN-LIKE (SPL) transcription factors (Xie et al., 2017, 2020). Subsequently, SPLs directly enhance expression of the floral integrators *SUPPRESSOR OF OVEREXPRESSION OF CONSTANS 1* (*SOC1*) and *FT*, or indirectly through elevation of *microRNA172* (*miR172*) levels that inhibit *APETALA 2* (*AP2*)-like repressors of flowering (Zheng et al., 2019). Although the shade avoidance studies suggest a putative role for (F)R light in the regulation of flowering through the age pathway, the photoreceptors that are involved, and the underlying molecular mechanisms remain to be clarified. Moreover, LED studies are required to confirm if plant ageing can be regulated by light quality, and if this pathway can be exploited towards preferred flowering phenotypes.



Chapter 5: Light quality regulates flowering

As a follow-up of our experiments in **chapter 3**, we used LEDs to study the timing of the floral transition by changes in light quality in Arabidopsis, tomato, and lettuce plants. Treatment with monochromatic red light resulted in late flowering in LD Arabidopsis and lettuce plants, but not in DN tomato and lettuce plants. Moreover, Arabidopsis plants grown in the red LED condition failed to establish *CO* and *FT* peaks at the end of the day, which confirmed that blue light must be present in the spectrum to activate the photoperiodic pathway in this species. In contrast, treatment with monochromatic blue light caused early flowering in LD plant species, as well as in a DN lettuce accession. Expression analysis of *GI*, *miR156*, *miR172*, *SPLs*, *FT* and *SOC1* revealed that early flowering in the blue LED condition resulted in part from a lack of PHYB-dependent inhibition of the age pathway. In conclusion, we showed that the age pathway is repressed by the presence of red light in the spectrum, thereby revealing a long sought-after photoperiod-independent function for PHYB in the inhibition of flowering.

Results

Shoot development is greatly influenced by red and blue light in Arabidopsis, but not in tomato.

In **chapter 3** we observed that Arabidopsis development is greatly influenced by light quality. Although many traits were influenced by red or blue light, the most intriguing phenotype was observed in the shoot of Arabidopsis plants. To follow up, we performed weekly imaging of Arabidopsis plants grown in

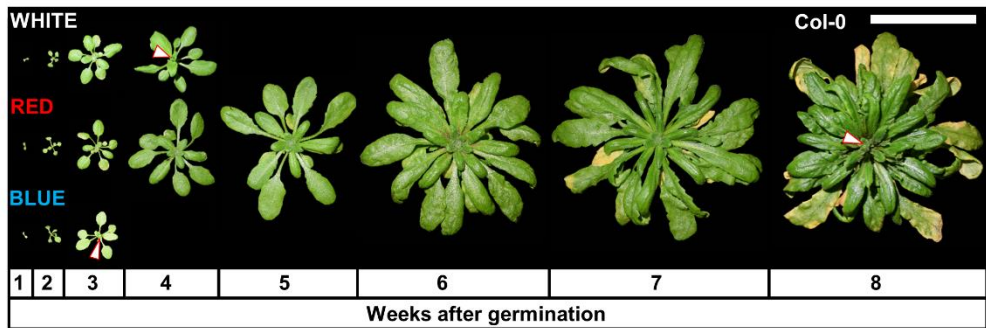


Figure 1: Arabidopsis shoot development is greatly influenced by red and blue light.












Representative Arabidopsis plants of ecotype Columbia (Col-0) that were grown in white, red, or blue LED conditions. Plants were photographed every week from 7 days after germination until bolting. For presentation purposes, rosettes were object selected and copy/pasted on a black background using ImageJ (Fiji) software. White arrowheads indicate the first visible flower buds. The scale bar indicates 5 cm. Similar results were obtained in three independent experiments.

white, red, or blue LED conditions (**Figure 1**). In white LED light, rosette leaf numbers (14 ± 0.3) and flowering time (24 ± 0.5 days) resembled development of Arabidopsis plants grown under regular fluorescent tube lighting systems (**Figure 1 (top panel), Figure 2A**). Plants that were grown in monochromatic red light developed large rosettes (42 ± 0.4 leaves) and flowered extremely late (48 ± 0.7 days), resembling Arabidopsis development under SD conditions in white light (**Figure 1 (middle panel), Figure 2A**). In contrast, treatment with monochromatic blue light resulted in small rosettes ($5-6 \pm 0.1$ leaves) and very early flowering (15 ± 0.4 days) (**Figure 1 (bottom panel), Figure 2A**). Treatment with monochromatic red light resulted in a remarkable decrease in plastochron (flowering time divided by the total number of rosette leaves: 1.1



Table 1: Arabidopsis leaf heteroblasty is altered in monochromatic blue light.

Leaf morphology, length/width (L/W) ratio (\pm SE, $n=10$) of the leaf blades, and appearance of abaxial trichomes of *Arabidopsis Columbia* (Col-0) plants that were grown in white, red, or blue LED conditions. For presentation purposes, leaf images were changed into black and white images using ImageJ (Fiji) software. Monochromatic LED conditions (red or blue) were compared to white (control) using a two-sided Student's *t*-test (asterisks indicate significant differences * $p<0.05$). Similar results were obtained in two independent experiments.

LED CONDITION	TRAIT	LEAF #1	LEAF #3	LEAF #5	LEAF #7
WHITE	Morphology				
	L/W ratio	1.14 \pm 0.01	1.25 \pm 0.03	1.54 \pm 0.04	1.76 \pm 0.05
	Abaxial trichomes	No	No	No	Yes
RED	Morphology				
	L/W ratio	1.10 \pm 0.01	1.23 \pm 0.04	1.51 \pm 0.05	1.75 \pm 0.05
	Abaxial trichomes	No	No	No	Yes
BLUE	Morphology				N/A
	L/W ratio	*1.21 \pm 0.01	*1.38 \pm 0.04	*1.89 \pm 0.05	N/A
	Abaxial trichomes	No	No	No	N/A

days) compared to white light (1.8 days), whereas plastochron was significantly increased in monochromatic blue light (2.8 days) (**Figure 2B**). Confocal imaging of shoot apices of *Arabidopsis pDR5::GFP* plants showed that, compared to white light, the shoot apex was significantly enlarged in the red LED condition, and significantly reduced in the blue LED condition (**Figure 2C, D**). Moreover, in the blue LED condition, the relative *pDR5::GFP* signal in the shoot meristem was significantly reduced compared to white and red LED conditions (**Figure 2E**). Leaf blade measurements revealed that



rosette leaves of plants grown in monochromatic blue light had a significantly higher length/width ratio, when compared to white or red LED conditions (**Table 1**), suggesting early vegetative phase change (VPC). However, no abaxial trichomes were present on rosette leaves of plants grown in monochromatic blue light (**Table 1**), whereas in the white and red LED conditions they were indicative of VPC around leaf number 6 or 7. Interestingly, we did not observe any differences in tomato compound leaf numbers, plastochron, shoot meristem size, or *pDR5::YFP* signals between the LED conditions (**Figure S1**). In summary, this data implied that red and blue light have an antagonistic effect on leaf initiation and growth of Arabidopsis, but not of tomato plants.

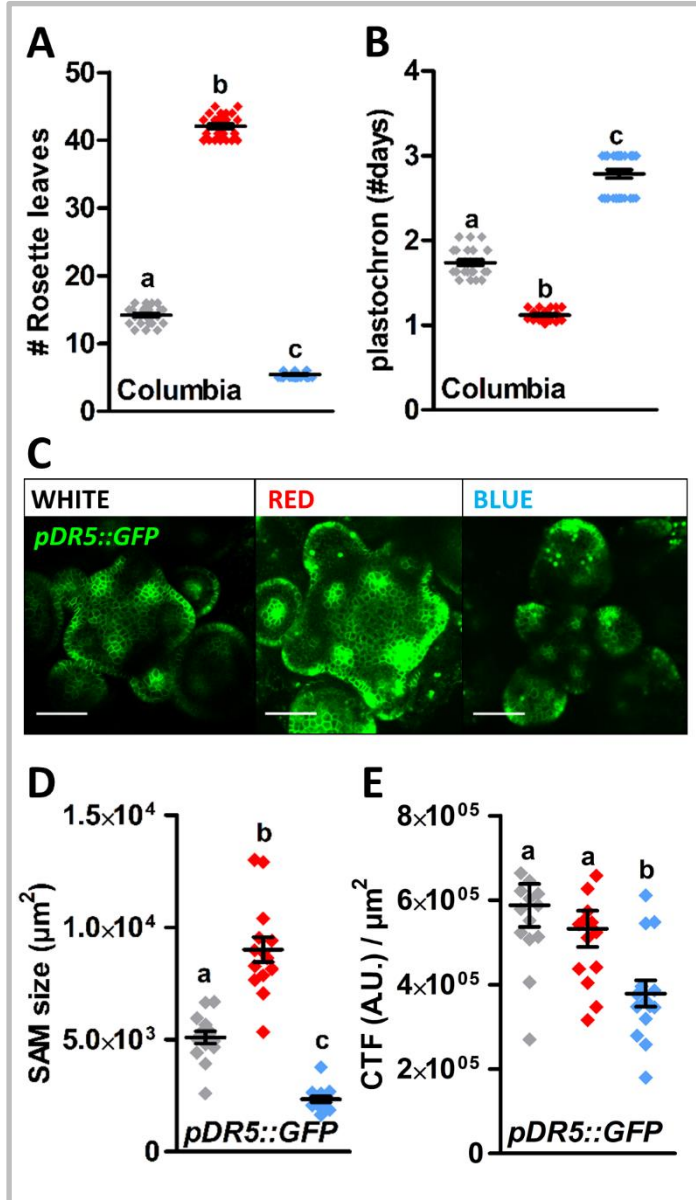
Late flowering in monochromatic red light is caused by inactivation of the photoperiodic pathway.

Because we previously observed that light quality affects flowering of LD Arabidopsis plants, but not of DN tomato plants (**chapter 3**), we next investigated the key photoreceptors involved in the photoperiodic pathway: the Zeitlupe family. Analysis of Arabidopsis *ztl*, *fkf1*, and *lkp* mutants showed a significant delay in flowering of the mutants compared to wild-type plants in both white and blue LED conditions. In monochromatic red light, flowering time of the mutants was similar to that of wild-type plants, confirming that the presence of blue light in the spectrum, perceived by the ZTL family of photoreceptors, is required to promote flowering (**Figure 3A**). Next, we investigated the diurnal expression patterns of *GI*, *CO*, and *FT* in 14-day-old wild-type Arabidopsis plants grown in the different LED conditions. In white light, expression of *GI* peaked around Zeitgeber time (ZT) 9, which induced



Chapter 5: Light quality regulates flowering

CO peaks around ZT12 and ZT18. Subsequently, the presence of a *CO* peak at the end of the day promoted *FT* expression around ZT15 (**Figures 3B-D**). In monochromatic red light, the *GI* peak was significantly reduced compared to white light (**Figure 3B**). As a likely result of this, plants grown in the red LED condition failed to establish the *CO* peaks that would induce *FT* expression (**Figures 3C, D**). This explains why LD Arabidopsis plants, that were grown in monochromatic red light, develop similar to SD grown plants. In monochromatic blue light, peaks in *GI* and *CO* expression occurred simultaneously with, but were significantly higher than, those of white light-grown plants (**Figures 3B, C**). *FT*





expression levels were significantly higher at all time points in blue LED conditions. In addition, the *FT* expression levels peaked throughout a longer period of time (**Figure 3D**), hence the extremely early flowering. To investigate if photoperiod-sensitivity is required for regulation of the floral

Figure 2: Red and blue light act antagonistically on organ formation at the shoot apical meristem in Arabidopsis.

A. Rosette leaf number until flowering of Arabidopsis Columbia (Col-0) plants grown in white, red, or blue LED conditions. **B.** Plastochron length (number of rosette leaves divided by the days until flowering) of Col-0 plants grown in the different LED conditions. **C.** Confocal images of representative shoot apices of Arabidopsis *pDR5::GFP* plants grown in the different LED conditions. **D.** Shoot apical meristem (SAM) surface area (in μm^2) of Arabidopsis *pDR5::GFP* plants grown in the different LED conditions. **E.** Corrected Total Fluorescence (CTF) of the *pDR5::GFP* signal in Arbitrary Units (A.U.) in shoot apices of Arabidopsis plants grown in the different LED conditions. Graph colours represent white, red, or blue LED conditions in **A**, **B**, **D** and **E**. Scale bars indicate 50 μm in **C**. LED conditions were compared using a one-way ANOVA followed by a Tukey's test (letters **a**, **b**, and **c** indicate statistically significant differences, $p < 0.05$) in **A**, **B**, **D** and **E**. Error bars represent standard error from mean in **A**, **B**, **D** and **E**. Similar results were obtained in two independent experiments.

transition by red or blue light, we compared the development of LD Arabidopsis and DN tomato plants to two lettuce accessions with different photoperiod-sensitivities: Meikoningin (LD) and Gaardenier (DN) (**Figure S2**). In LD lettuce plants, we observed early flowering in monochromatic blue light, and late flowering in monochromatic red light (**Figures 4A, B**).

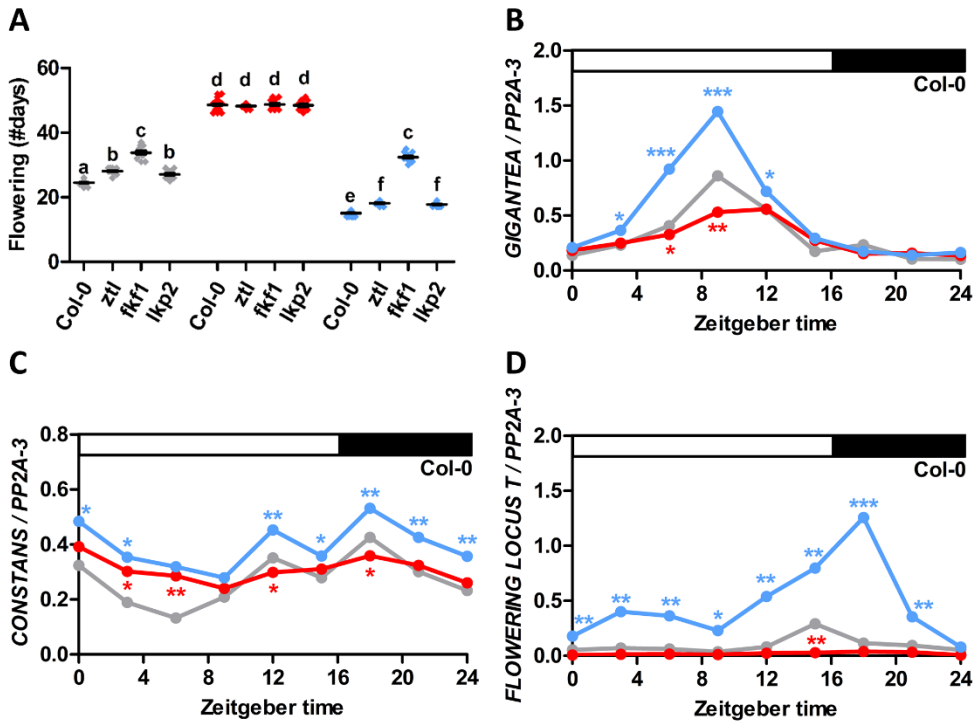


Figure 3: The Arabidopsis photoperiodic pathway is inactive in spectra that lack blue light.

A. Flowering time of Arabidopsis Columbia (Col-0) and photoreceptor mutants *ztl*, *fkl1* and *lkp2* grown in white, red, or blue LED conditions. **B-D.** Diurnal gene expression patterns of *GIGANTEA* (**B**), *CONSTANS* (**C**) and *FLOWERING LOCUS T* (**D**) in 14-day-old wild-type Arabidopsis plants that were grown in white, red, or blue LED conditions. Graph colours represent the different LED conditions. LED conditions and wild types or mutants were compared using a one-way ANOVA followed by a Tukey's test (letters **a**, **b**, **c**, **d**, **e**, and **f** indicate statistically significant differences, $p < 0.05$) in **A**. In **B-D**, monochromatic LED conditions (red or blue) were compared to white (control) using a two-sided Student's *t*-test (asterisks indicate significant differences at a specific time point (** $p < 0.01$, *** $p < 0.001$, * $p < 0.05$)). For presentation purposes, not all time points that were significantly different between white and red LED conditions (**Table S3**) were labelled with asterisks in **D**. Error bars represent standard error from mean in **A** ($n = 30$), standard errors and *p*-values for **B-D** are listed in **Table S3**. Similar results were obtained in three independent experiments.

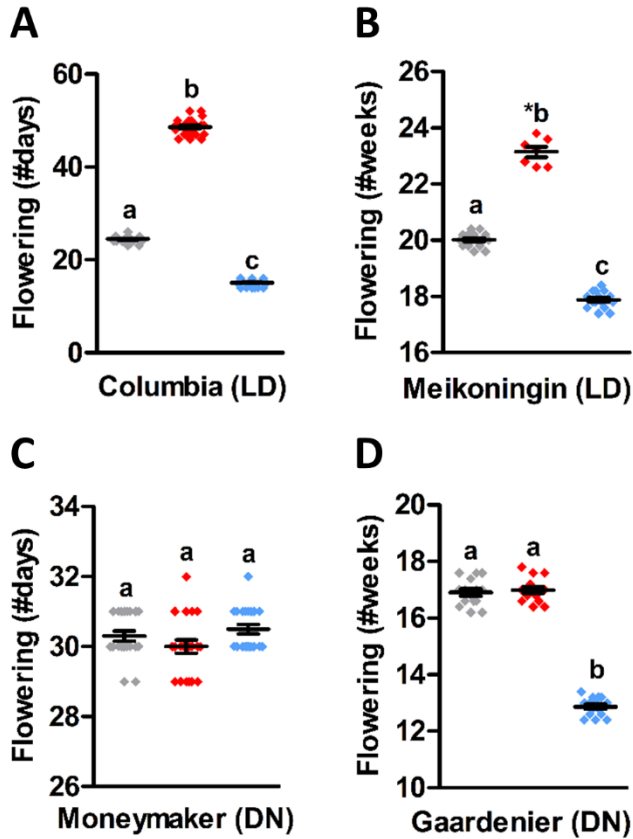


Figure 4: Late flowering in monochromatic red light relies on day length sensitivity.

A-B. Flowering time of long-day (LD) plants: *Arabidopsis* ecotype Columbia (**A**), and lettuce variety Meikoningin (**B**) grown in white, red, or blue LED conditions. **C-D.** Flowering time of day-neutral (DN) plants: tomato cv. Moneymaker (**C**), and lettuce variety Gaardenier (**D**) grown in the different LED conditions. Graph colours represent the different LED conditions. LED conditions were compared using a one-way ANOVA followed by a Tukey's test (letters **a**, **b**, and **c** indicate statistically significant differences, $p < 0.05$). Error bars represent standard error from mean. Similar results were obtained in two (**B/D**) or three (**A/C**) independent experiments.



As expected, late flowering in the red LED condition was lost in DN lettuce plants. Interestingly, early flowering in monochromatic blue light was observed in DN lettuce plants, but not in DN tomato plants (**Figures 4C,D**). The combined data of Arabidopsis, tomato, and lettuce suggested that late flowering in monochromatic red light relies mainly on inactivation of the blue light Zeitlupe photoreceptor-driven photoperiodic pathway, and can thus be observed in LD, but not in DN plant species.

Early flowering in monochromatic blue light is caused by upregulation of the age pathway.

We observed early flowering in the DN lettuce cultivar Gaardenier plants that were grown in monochromatic blue light (**Figure 4D**), which suggested that in these plants, flower induction relies on a flowering pathway other than the photoperiodic pathway. The increased plastochron, length/width ratios of the leaf blade and enhanced *GI* expression that we observed in Arabidopsis plants grown in the blue LED condition together pointed towards the age pathway (Jung et al., 2007; Wang et al., 2008; Wu et al., 2009). To investigate this, we focused on expression of known regulators of VPC in the rosettes of 5- to 15-day-old Arabidopsis plants grown in the different LED conditions. The expression of *miR156* was significantly reduced in monochromatic blue light, compared to white and monochromatic red light (**Figure 5A**). As a likely result, gene expression levels of *miR172*, *SPL2*, *SPL9*, *SPL10*, *SPL11*, and *SPL15* were significantly higher in the blue LED condition than in the other LED conditions (**Figures 5B, D, E, F, G, I**). The expression of the newly identified plant longevity gene *AHL15* (Karami et al., 2020; Rahimi et al., 2022) was not altered in monochromatic blue light, but was significantly

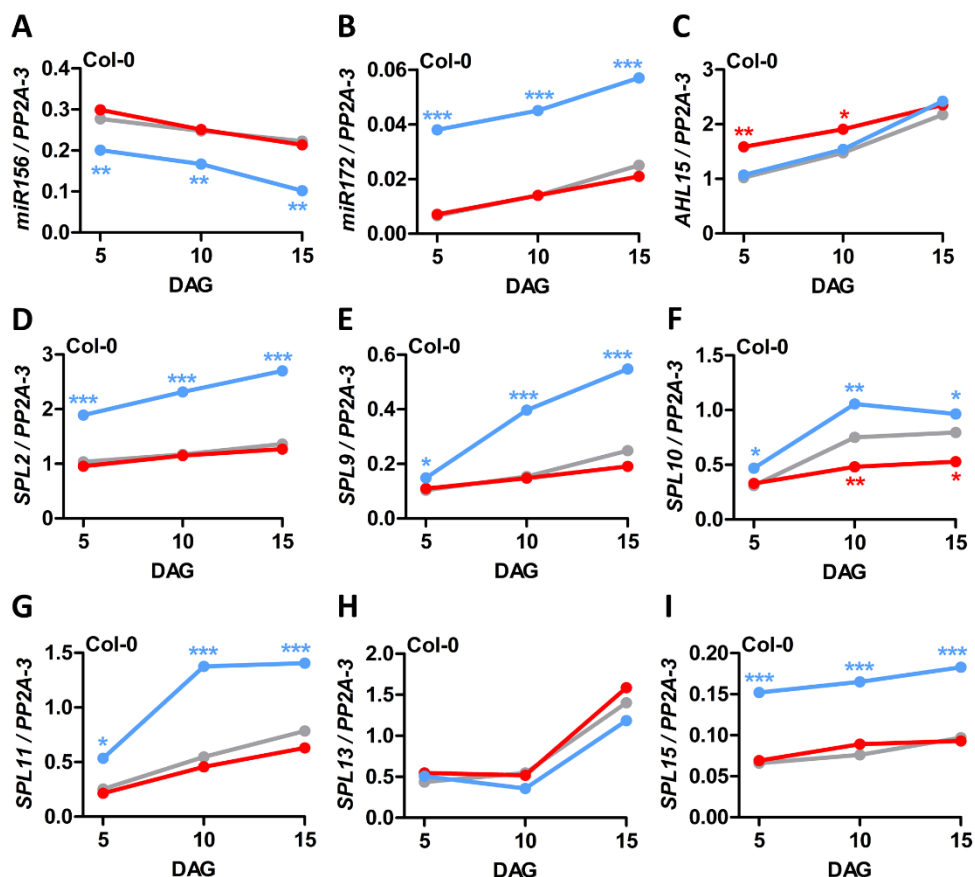


Figure 5: The Arabidopsis age pathway is promoted in spectra that lack red light.

A-I. Quantitative RT-PCR analysis of genes involved in the age pathway in Arabidopsis plants of ecotype Columbia (Col-0) grown in white, red, or blue LED conditions. Relative expression levels of *miR156* (**A**), *miR172* (**B**), *AHL15* (**C**), *SPL2* (**D**), *SPL9* (**E**), *SPL10* (**F**), *SPL11* (**G**), *SPL13* (**H**), and *SPL15* (**I**) at 5, 10 and 15 days after germination (DAG). Graph colours represent the different LED conditions. Monochromatic LED conditions (red or blue) were compared to white (control) using a two-sided Student's *t*-test (asterisks indicate significant differences at a specific time point (***p*<0.001, ***p*<0.01, **p*<0.05)). Standard errors and *p*-values are listed in **Table S3**. Similar results were obtained in three independent experiments.



higher in 5- and 10-day-old plants grown in monochromatic red light (**Figure 5C**). Expression of *SPL10* was significantly decreased in 5- to 15-day-old Arabidopsis plants grown in monochromatic red light (**Figures 5F and 6D**), whereas the expression of all other *SPLs* was similar in the white and red LED conditions. *SPL4*, *SPL6*, and *SPL13* expression levels were indifferent to the LED conditions (**Figures 5H and S3A-D**). For *SPL5*, gene expression was significantly higher in monochromatic blue light, compared to white and monochromatic red light, but its overall expression levels were extremely low (**Figure S3B**). Analysis of the expression of *SPL2*, *SPL3*, *SPL9*, *SPL10*, *SPL11*, and *SPL15* at 10-25 days after germination, which comprises the floral transition in monochromatic blue and white light-grown plants, showed again a significant increase of these age pathway genes in monochromatic blue light (**Figure 6A-F**). Because the same *SPL* genes already showed elevated expression in 5- to 15-day-old plants grown in monochromatic blue light, whereas expression of the floral integrators *FT* and *SOC1* was only elevated in 15- and 20-day-old plants (**Figure 6G, H**), it is likely that early flowering in monochromatic blue light results from increased *SPL* expression. To confirm this, we tested mutant plant lines with reduced (*spl9spl15* or *p35S::miR156*) or enhanced (*p35S::MIM156*) *SPL* expression levels. Flowering of *p35S::miR156* or *spl9 spl15* double mutant plants was delayed in the white and blue LED conditions, compared to wild-type plants, whereas *p35S::MIM156* plants flowered earlier than wild-type in white light, and later than wild-type in monochromatic blue light (**Figure S3E**). In monochromatic red light, flowering time of all three lines was similar to wild-type plants, corroborating our previous conclusion that late flowering in monochromatic red light relies largely on the absence of blue light-stimulation of the photoperiod pathway

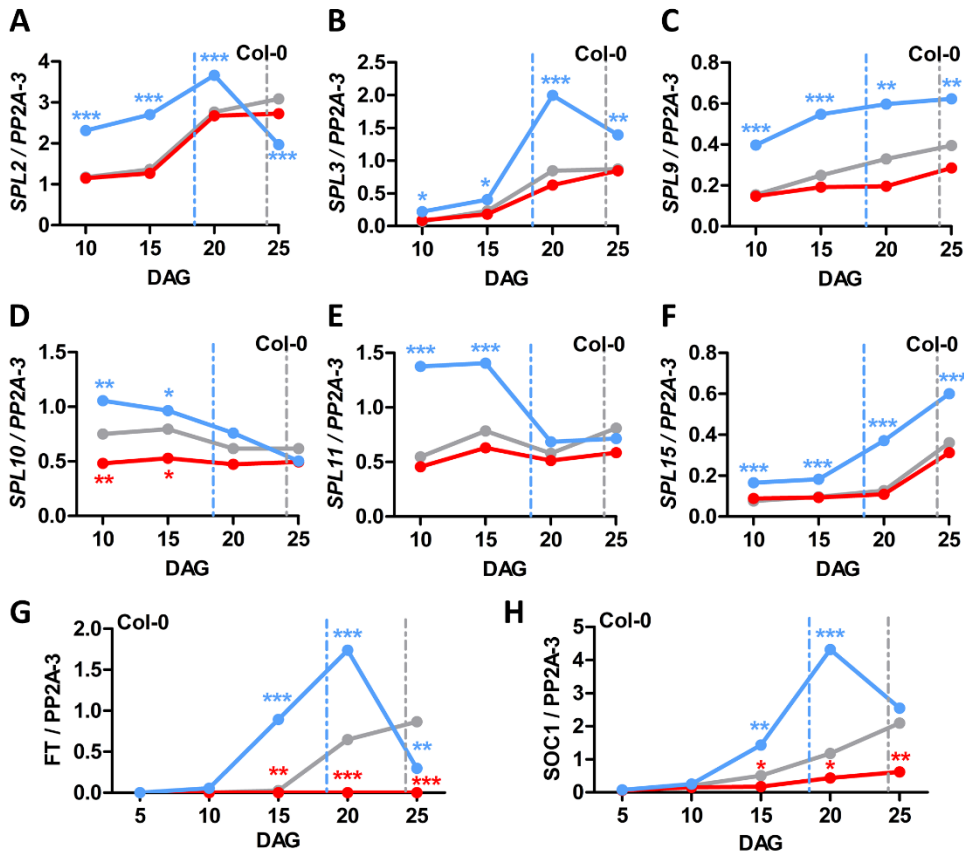


Figure 6: Early flowering in spectra that lack red light results from accelerated ageing.

A-F. Quantitative RT-PCR analysis of *SPL* genes that induce flowering in Arabidopsis Columbia (Col-0) plants that were grown in white, red, or blue LED conditions at 10, 15, 20, and 25 days after germination (DAG). Relative expression levels of *SPL2* (A), *SPL3* (B), *SPL9* (C), *SPL10* (D), *SPL11* (E) and *SPL15* (F). **G-H.** Quantitative RT-PCR analysis of the floral integrators *FT* (G) and *SOC1* (H) in Col-0 plants that were grown in different LED conditions at 5, 10, 15, 20, and 25 DAG. Graph colours represent the different LED conditions, dashed lines represent the moment of bolting. Monochromatic LED conditions (red or blue) were compared to white (control) using a two-sided Student's *t*-test (asterisks indicate significant differences at a specific time point (****p*<0.001, ***p*<0.01, **p*<0.05)). Standard errors and *p*-values are listed in **Table S3**. Similar results were obtained in three independent experiments.



(**Figure S3E**). Interestingly, the flowering time of *p35S::miR156*, *p35S::MIM156* and *spl9 spl15* double mutant in monochromatic blue light did not significantly differ from that of wild-type plants flowering in white light (**Figure S3E**), suggesting that disruption of the *miR156-SPL* module of the age pathway results in a (partial) rescue of the early flowering phenotype in the blue LED condition. Our quantitative RT-PCR data, together with flowering time analysis, suggests that shoot meristems age faster in monochromatic blue light, ultimately resulting in early flowering.

In spectra that contain red light, Arabidopsis PHYB inhibits flowering by repressing the age pathway.

The results described above suggest that shoots of plants grown in monochromatic blue light (thus lacking red light in the spectrum) mature early compared to those grown in white or red LED conditions, implying that red light actively inhibits the age pathway. To investigate this, we analysed photoreceptors of the red/FR light-sensitive phytochrome (PHY) family. Analysis of *phyA*, *phyB*, *phyC*, *phyD*, and *phyE* single mutants showed a significant early flowering of *phyB* mutants compared to wild type or other *phy* mutant plants in both white and red LED conditions, and to a lesser extent, in the blue LED condition (**Figure 7A**), suggesting a putative role for PHYB in inhibition of plant ageing. Since PHYB has been proposed to repress *GI* expression, which promotes *miR172* (Huq et al., 2000; Jung et al., 2007), we analysed its expression in *phyB* plants grown in the different LED conditions. Expression of *GI* was similar in *phyB* plants grown in white and monochromatic blue light, thus further supporting the PHYB-GI interaction, and possibly explaining the elevated diurnal *GI* expression in Col-0 plants



grown in monochromatic blue light (**Figure 3B**). However, its expression was significantly lower in 15-day-old *phyB* plants grown in red light (**Figure 7B**), which is most likely a side-effect of inactivation of the photoperiodic pathway in this LED condition. Next, we investigated the plant ageing regulators that were differentially expressed in wild-type plants grown in monochromatic blue light, compared to red or white light (**Figure 5**). Except for *SPL10* expression in the red LED condition, the differential expression of *miR156*, *miR172*, *SPL2*, *SPL9*, *SPL11*, and *SPL15* in the different LED conditions was lost in *phyB* plants (**Figures 7C-I**). This suggests that, in wild-type plants, the differential expression of these ageing regulators between the blue LED condition and the white or red LED conditions relies on PHYB activation. To summarise, our data suggests that, in the LD plant *Arabidopsis*, PHYB signalling suppresses the age pathway through *miRNAs*, *SPLs*, and *GI* in response to the presence of red light in the spectrum.

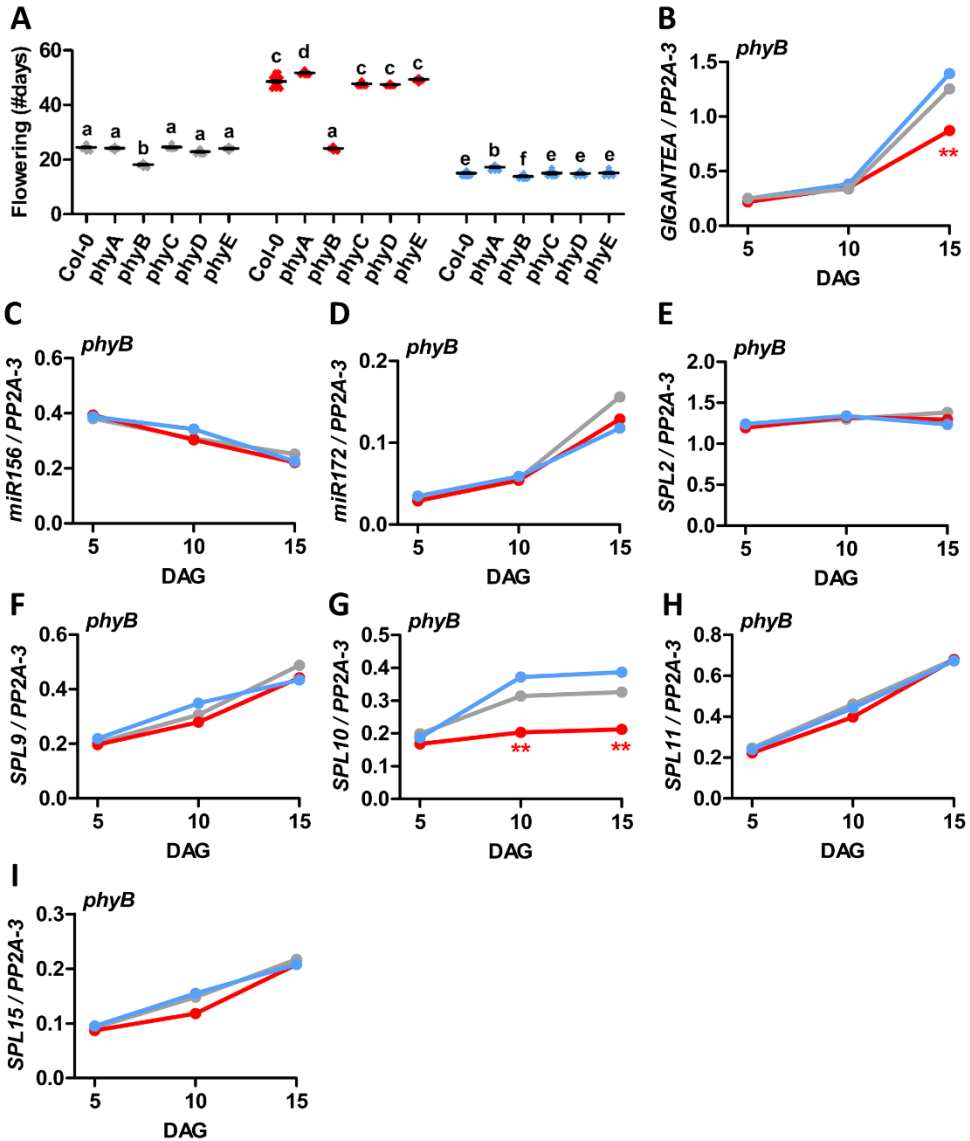
Discussion

In **chapter 3**, we observed that *Arabidopsis* shoot development is greatly influenced by light quality, whereas tomato shoots remained indifferent to red or blue light. Here, we further investigated the formation of *Arabidopsis* and tomato shoot organs, and their correlation to flowering time. *Arabidopsis* plants grown in monochromatic red light developed more rosette leaves, and at a higher pace, which correlated to a large shoot apex, and an extended vegetative phase caused by late flowering. In contrast, *Arabidopsis* plants grown in monochromatic blue light developed only a few leaves and at a



Chapter 5: Light quality regulates flowering

significantly slower rate than white- or red light-grown plants. In addition to a small shoot apex and a shortened vegetative phase due to extremely early flowering, the auxin response in the shoot apex was decreased in the blue LED condition. Interestingly, in tomato plants, leaf number, plastochron, flowering





time, and size of, and auxin response in, the shoot meristem were all indifferent to monochromatic red and blue light treatments. Since *Arabidopsis* is a LD plant, and tomato a DN species, we aimed to explain this difference by investigating the photoperiodic pathway. In monochromatic red light (thus

Figure 7: *Arabidopsis* PHYB inhibits flowering by repressing the age pathway.

A. Flowering time of *Arabidopsis* Columbia (Col-0) and photoreceptor mutants *phyA*, *phyB*, *phyC*, *phyD*, and *phyE* grown in white, red, or blue LED conditions.

B-I. Quantitative RT-PCR analysis of genes involved in the age pathway in Col-0 and *phyB* plants grown in the different LED conditions. Relative expression levels of *GIGANTEA* (**B**), *miR156* (**C**), *miR172* (**D**), *SPL2* (**E**), *SPL9* (**F**), *SPL10* (**G**), *SPL11* (**H**), and *SPL15* (**I**) at 5, 10, and 15 days after germination (DAG). Graph colours represent the different LED conditions. LED conditions and wildtypes or mutants were compared using a one-way ANOVA followed by a Tukey's test (letters **a**, **b**, **c**, **d**, **e**, and **f** indicate statistically significant differences, $p < 0.05$) in **A**. In **B-I**, monochromatic LED conditions (red or blue) were compared to white (control) using a two-sided Student's *t*-test (asterisks indicate significant differences at a specific time point (** $p < 0.01$)). Error bars represent standard error from mean in **A** ($n=30$), standard errors and *p*-values for **B-I** are listed in **Table S3**. Similar results were obtained in three independent experiments.



Chapter 5: Light quality regulates flowering

lacking blue light in the spectrum), the inactivity of photoreceptors of the Zeitzlupe family resulted in a significant decrease in *GI* and *CO* expression, and thus Arabidopsis plants failed to establish a peak in *FT* expression at the end of the day to induce flowering. Although *GI*, *CO*, and *FT* levels were significantly elevated in Arabidopsis plants grown in the blue LED condition, early flowering of a DN lettuce accession in monochromatic blue light suggested that this phenotype could be photoperiod-independent. Gene expression analysis of components of the age pathway showed that *miR156*, *miR172*, *SPL2*, *SPL3*, *SPL9*, *SPL10*, *SPL11*, and *SPL15* were differentially expressed in monochromatic blue light (thus lacking red light in the spectrum), when compared to white and red LED conditions. Subsequently, *SOC1* and *FT* levels were elevated in 15- to 25-day-old Arabidopsis plants grown in the blue LED condition, suggesting that the presence of red light in the spectrum is required to repress the age pathway and thereby delay VPC and flowering. In addition to early flowering, *phyB* mutants lost the differential expression of *miR156*, *miR172*, *SPL2*, *SPL9*, *SPL10*, *SPL11*, and *SPL15* between the white and blue LED conditions, confirming that PHYB represses the age pathway in light spectra that contain red light.

Light quality regulates shoot organ formation and morphology.

The rosette phenotype of Arabidopsis plants grown in the different LED conditions resulted from changes in flowering time and plastochron, that correlated to significant differences in shoot apex size. The accumulation of stem cells in the meristem determines its size, and is regulated by *CLAVATA* (*CLV*) genes that have been shown to respond to changes in photoperiod (Jeong and Clark, 2005). Therefore, the altered meristem size of Arabidopsis plants



grown in monochromatic red or blue light likely correlates to changes in photoperiodic regulation. This hypothesis was further supported by the complete indifference of DN tomato apices to these light treatments. Interestingly, we also observed a decreased auxin response in *Arabidopsis* shoot apices of plants grown in monochromatic blue light, that was not observed in tomato shoot apices. Since auxin regulates the initiation of new leaf primordia (Lee et al., 2019), this decrease in auxin response suggested that, similar to a dark treatment, the blue LED condition somehow interferes with PIN1-dependent auxin flux in the shoot apex (Yoshida et al., 2011). This implies that there are either functional differences in auxin-dependent primordia initiation between *Arabidopsis* and tomato, or that auxin responses in the shoot apex may be (partially) photoperiod-sensitive in LD plants, and thus indifferent to red or blue light in DN species. Aside from initiation and outgrowth of new leaves, monochromatic blue light treatment of *Arabidopsis* plants also affected the morphology of rosette leaves. Leaf blades of plants grown in this LED condition had a significantly higher length/width (L/W) ratio than those of plants grown in white or red LED conditions, and even reached beyond 1.7, which is indicative of adult leaves (Telfer et al., 1997). However, these leaves did not show other characteristics of adult leaves such as abaxial trichomes, or serrated margins. Based on leaf heteroblasty, these plants would thus not be identified as adult vegetative, suggesting that VPC was incomplete in these plants. By definition, VPC is described as the acquisition of flowering competence (Huijser and Schmid, 2011), which implies that all reproductive plants have completed this developmental phase transition. However, *Arabidopsis* plants grown in the blue LED condition already flowered after the production of only 5-6 leaves that lacked most adult



Chapter 5: Light quality regulates flowering

characteristics. Therefore, we speculate that either the widely used leaf heteroblasty characteristics are not completely reliable for the identification of adult vegetative plants, or that plants become reproductive after a (partially) incomplete VPC when grown in monochromatic blue light. Although VPC and the floral transition are uncoupled in woody species (Huijser and Schmid, 2011), this is not common for *Arabidopsis*. However, leaf heteroblasty of white- and monochromatic red light-grown plants suggested that VPC occurs simultaneously in these LED conditions, while their floral transition occurs at different time points, indicating that spectra that lack blue light specifically delay the floral transition, independent of VPC.

Light quality regulates photoperiodic flowering.

In the past decades, many flowering studies have been conducted in photoperiod-sensitive LD and SD species to show that blue light photoreceptors of the *Zeitlupe* and cryptochrome families, and red/FR light-responsive phytochromes regulate photoperiodic flowering (Wu and Hanzawa, 2014). However, their responses had not been tested in LED lighting setups that simultaneously modulate multiple photoreceptors, and their putative interactions. Therefore, we analysed *Arabidopsis* photoreceptor mutants of the *Zeitlupe* family in the three LED conditions to confirm that the flowering response of these photoreceptors is only activated in spectra that contain blue light. Upon photoactivation, these photoreceptors interact with *GI* to inhibit CDFs and thereby alleviate their repression of *CO*, subsequently resulting in upregulation of the floral integrator *FT* (Samach et al., 2000; Sawa et al., 2007; Fornara et al., 2009). Our analysis of diurnal expression patterns confirmed that the presence of blue light is required in the spectrum to promote *GI*, *CO*,



and *FT* to induce flowering. Moreover, since flowering of DN tomato and lettuce accessions was indifferent to treatment with monochromatic red light, we showed that spectra that contain blue light can only promote flowering in photoperiod-sensitive species. In contrast to the red LED condition, *Arabidopsis* plants grown in white or monochromatic blue light did establish sufficient *GI* and *CO* expression to induce an end-of-day *FT* peak. Although FR light-activated PHYA has been shown to promote flowering as well (Valverde et al., 2004), we showed that FR light is not necessarily required to induce the photoperiodic pathway in LD plants. While elevated *FT* expression in monochromatic blue light, compared to white light, could have resulted from a previously described role for PHYB in targeted CO protein degradation (Valverde et al., 2004; Lazaro et al., 2015), a PHYB-GI interaction has been suggested as well (Huq et al., 2000). In conclusion, we verified that the presence of blue light in the spectrum, through activation of the Zeitzlupe photoreceptor family, promotes photoperiodic flowering. Our results suggest that, although flower-promoting roles for PHYA and CRY2 and a flower-inhibiting role for PHYB have been described, their role in photoperiodic flowering appears to be subordinate (**Figure 8**).

Light quality regulates plant ageing.

In addition to altered leaf heteroblasty of *Arabidopsis* plants grown in monochromatic blue light, we observed early flowering, not only in both LD species, but also in the DN lettuce accession, suggesting that the absence of red light in this spectrum promotes flowering in a photoperiod-independent manner. These results led us to further investigate the age pathway. Upregulation of five out of six VPC-associated *SPL* genes in plants grown in



Chapter 5: Light quality regulates flowering

monochromatic blue light, which combined with the increased L/W ratio of their rosette leaves, strongly suggested early VPC. The subsequent increase in *FT* and *SOC1* expression and flowering analysis of the *spl9 spl15* double mutant and *p35S::miR156* and *p35S::MIM156* lines confirmed the correlation between the miR156-SPL module and early flowering in monochromatic blue light. Altogether, this

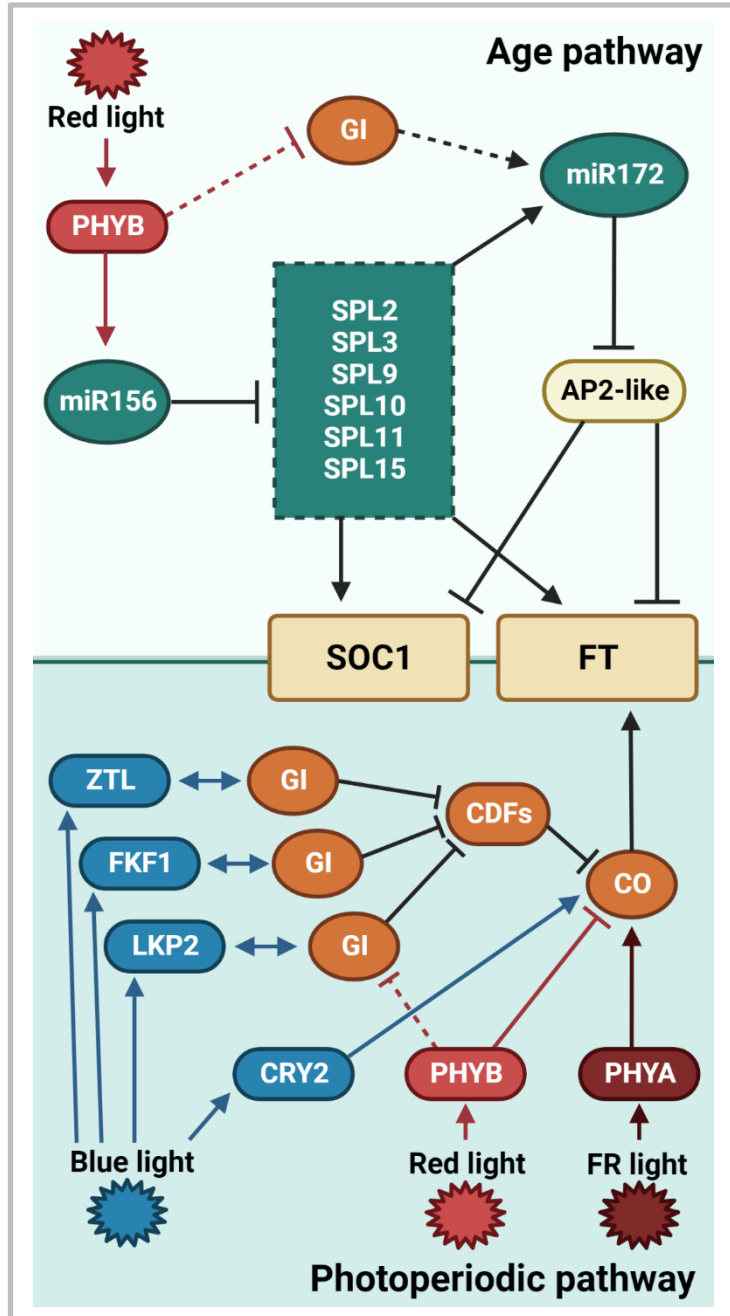




Figure 8: Model for regulation of the Arabidopsis floral transition by light quality.

The floral transition in Arabidopsis is regulated by light quality through both the age pathway (top) and the photoperiodic pathway (bottom). In spectra that contain red light, PHYB inhibits flowering through the age pathway in two ways: (1) PHYB promotes *miR156*, thereby enhancing its repression of *SPLs*, which reduces both their direct and indirect (through *miR172*) promotion of *SOC1* and *FT*. (this work) (2) We hypothesise an additional red light response where PHYB inhibits *GI* expression, thereby reducing its activation of *miR172*, which may lead to accumulation of AP2-like transcription factors that inhibit floral integrators *SOC1* and *FT* (this work; Huq et al., 2000; Jung et al., 2007). Furthermore, light quality regulates flowering through the photoperiodic pathway. In spectra that contain blue light, photoreceptors of the Zeirlupe family (ZTL, FKF1, and LKP2, this work) and CRY2 (Liu et al., 2008) promote flowering by modulation of *CO*, either directly (CRY2), or indirectly through complex formation with *GI* (Zeirlupes) that inhibits CDFs which repress *CO* expression. In addition, far-red (FR) light promotes *CO* expression through PHYA (Valverde et al., 2004). In spectra that contain red light, photoperiodic flowering is inhibited through PHYB-dependent degradation of CO proteins, and possibly also by decreasing *GI* expression (Valverde et al., 2004, this work, Huq et al, 2000). If modulation of CO levels by light quality leads to a CO peak at the end of the day, its subsequent promotion of *FT* is sufficient to induce flowering.

suggested that, in white and red LED conditions (where red light is present in the spectra), the age pathway is inhibited to delay both VPC and the floral transition, whereas this inhibition does not occur in the blue LED condition (that lacks red light in the spectrum). Based on early flowering of *phyB* in white and monochromatic red light, and on the fact that *phyB* mutants flower early both under inductive LD photoperiods, and non-inductive SD



Chapter 5: Light quality regulates flowering

photoperiods (Reed et al., 1993), we selected PHYB as a putative inhibitor of plant ageing. In *phyB* mutants, components of the miR156-SPL module were no longer differentially expressed in monochromatic blue light, thus confirming inhibition of the age pathway by PHYB. Although PHYB-promoted expression of *miR156* through degradation of PHYTOCHROME INTERACTING FACTORS (PIFs) has been described in a shade avoidance study (Xie et al., 2017), its effect on delaying VPC and flowering has not been reported yet. By revealing this long sought-after photoperiod-independent role for PHYB, we showed that light quality may be used to regulate VPC and flowering of some DN plant species, as well as LD plant species. In addition to regulation of the age pathway in a photoperiod-independent manner, a possible photoperiod-dependent function of PHYB in the age pathway should be considered as well. Diurnal *GI* expression levels in wild-type *Arabidopsis* plants grown in monochromatic blue light were significantly higher than in white light, however, in *phyB* mutants this difference was lost, thus further supporting the previously proposed PHYB-GI interaction (Huq et al., 2000). Interestingly, GI has been shown to promote *miR172* expression (Jung et al., 2007), supporting the possibility of a putative photoperiod-dependent role for PHYB in plant ageing (**Figure 8**). Surprisingly, DN tomato plants, in contrast to the DN lettuce accession, did not flower early in the blue LED condition. Since components of the age pathway have been identified in tomato (Zhang et al., 2011; Salinas et al., 2012; Li et al., 2013), a possible explanation for the indifference of tomato plants may be the lack of a true *PHYB* orthologue. Tomato *PHYB1* and *PHYB2* arose from an independent duplication in *Solanaceae* (Pratt et al., 1995), suggesting that PHYB function in plant ageing may not be conserved in *Solanaceae* species. To summarise, we showed that



the presence of red light in the spectrum is required for the activation of PHYB, which promotes *miR156*, resulting in decreased *SPL*, *FT* and *SOC1* expression that inhibits VPC and flowering (**Figure 8**).

Materials and Methods

Growth conditions and LED treatments

In all experiments, plants were grown at a 16h photoperiod, under white, deep red, or blue Philips Greenpower LED research modules (Signify B.V., Eindhoven, the Netherlands) with a measured photon flux density of $120 \pm 10 \mu\text{mol m}^{-2}\text{s}^{-1}$ at the top of the canopy, a temperature of 21°C, and 70% relative humidity. The percentages of blue, green, red, and far-red wavelengths for the different LED modules are listed in **Table S1** of **chapter 3**. Experiments with the different LED treatments were performed simultaneously in the same growth chamber in separate compartments enclosed by white plastic screens with a proximal distance of 50 cm to the plants.

Plant lines and seed germination

Experiments were performed with *Arabidopsis thaliana* (Arabidopsis) ecotype Columbia (Col-0), *Solanum lycopersicum* (tomato) cultivar Moneymaker (MM) and *Lactuca sativa* (lettuce) cultivars Meikoningin (long-day) or Gaardenier (day-neutral). Arabidopsis and tomato mutant or reporter lines that were used have been described before and are listed in **Table S1**. Arabidopsis mutant lines were genotyped using the primers listed in **Table S2**. Arabidopsis seeds were sown on the soil surface and stratified for 5 days at 4°C in darkness.



Chapter 5: Light quality regulates flowering

Subsequently the seeds were moved to white light to allow simultaneous germination. After one day in white light, the pots were placed in the LED conditions. Tomato and lettuce seeds were placed approximately 2 cm under the soil surface and the pots were directly placed in the LED conditions.

Analysis of leaf formation, morphology, and flowering time

Arabidopsis rosette leaves or tomato compound leaves were counted every week from the moment they were visible by eye, until the floral transition. Plastochron was calculated based on the number of leaves and the number of days until the floral transition. *Arabidopsis* rosettes were photographed every week, until bolting. At this time, individual rosette leaves were removed, flattened, and photographed for measurements to calculate the length/width ratio of the leaf blade. All measurements were performed with ImageJ (Fiji) (Schindelin et al., 2012). The individual rosette leaves were also analysed under a Leica MZ12 light microscope to score for the presence of abaxial trichomes. *Arabidopsis* flowering time was measured in number of days until bolting. For tomato, toothpicks were used to carefully push aside the young leaves from the apex. Flowering time was determined as the day on which small inflorescences became visible near the shoot apex. In lettuce plants, flowering was determined by the number of days until an inflorescence became visible above the head. At this time, representative tomato and lettuce plants were photographed.

Microscopic analysis of the shoot apex

Primary inflorescences of *Arabidopsis pDR5::GFP* plants at 1 week after bolting were dissected using 0.3 mm x 13 mm needles (#304000, BD



MicroalanceTM). All flowers, flower buds, and stage IV and V primordia were removed to expose the shoot apex. Dissected Arabidopsis shoot apices were mounted on a glass slide using 1% Low Melting Point (LMP) agarose (#16520050, Thermo ScientificTM). To visualise *pDR5::GFP*, a Zeiss LSM5 Exciter/Axiolmager equipped with a 40x water objective and a 488 nm argon laser with a 505-530 nm band pass filter was used. The shoots of 25-day-old tomato *pDR5::YFP* plants were dissected using tweezers. All leaves and primordia that were visible by eye were removed to expose the shoot apex. Dissected tomato shoot apices were mounted on a glass slide using 1% LMP agarose and imaged with a Leica MZ16FA equipped with a Leica DFC420C camera. YFP fluorescence was detected using a 510/20 nm excitation filter and a 560/40 nm emission filter. Based on the microscopic images, the meristem size of Arabidopsis and tomato was measured using ImageJ (Fiji) software. To quantify the fluorescent signals, the corrected total cell fluorescence (CTCF) method (McCloy et al., 2014) was slightly adjusted to quantify the corrected total fluorescence (CTF) of the shoot apex. $CTF = \text{integrated density} - (\text{area of shoot apex} * \text{mean fluorescence of background readings})$. For images of Arabidopsis shoot apices, the CTF was also corrected for the differences in SAM size between LED conditions.

RNA extraction and qRT-PCR

All tissues that were used for RNA extraction were frozen in liquid nitrogen directly after harvesting within their respective LED condition. For each experiment, five different plants from the same LED condition were pooled and used for RNA extraction. Three biological replicates were used for each plant line per LED condition, with three technical replicates. For analysis of



Chapter 5: Light quality regulates flowering

diurnal expression patterns, RNA was extracted from the rosettes of 14-day-old *Arabidopsis* plants, at the following time points: Zeitgeber time (ZT)0 (07.00), ZT3 (10.00), ZT6 (13.00), ZT9 (16.00), ZT12 (19.00), ZT15 (22.00), ZT18 (01.00), ZT21 (04.00) and ZT24 (07.00). For analysis of gene expression throughout development, RNA was extracted from the rosettes of 5-, 10-, 15-, 20-, or 25-day-old *Arabidopsis* plants (always at ZT9). Frozen tissue samples were ground with a TissueLyser II (#85300, Qiagen). Total RNA was extracted from the ground tissue using an RNeasy® Plant Mini kit (#74904, Qiagen), and used for first strand cDNA synthesis with the RevertAid First Strand cDNA Synthesis kit (#K1621, Thermo Scientific™). For miRNAs, total RNA was reverse transcribed with the SnoR101 reverse primer, and a miRNA-specific RT primer. For qRT-PCR, the cDNA was diluted 10x and used with TB Green Premix Ex Taq II (Tli RNase H Plus) (#RR820B, Takara) and the CFX96 Touch™ Real-Time PCR Detection System (#1855196, Bio-Rad). CT values were obtained using Bio-Rad CFX manager 3.1. The relative expression level of genes of interest was calculated according to the Livak method (Livak and Schmittgen, 2001), using *PP2A-3* (At2g42500) as a reference gene. All primers that were used for qRT-PCR experiments are listed in **Table S2**.

Statistical analysis and figures

For phenotypic analysis (leaf formation, flowering time), 20 tomato or lettuce plants, and 30 *Arabidopsis* plants were grown in each LED condition. For analysis of *Arabidopsis* leaf morphology, 10 representative biological replicates were used for each leaf number (1, 3, 5, and 7). For microscopic analysis of *Arabidopsis* and tomato shoot apices, images of 20 individual shoot apices were used to calculate meristem size and corrected total fluorescence



(CTF). In qRT-PCR experiments, rosettes of 10 individual plants were pooled for RNA extraction. For each data point, the mean of 3 cDNA samples, derived from 3 different RNA samples, was plotted in the graph. All data was obtained from either two (lettuce flowering, leaf morphology, microscopic analysis) or three independent experiments (phenotypic analysis of *Arabidopsis* and tomato, RT-qPCR). For phenotypic and microscopic analysis, the different LED conditions, or wild types and mutants, were compared using a one-way ANOVA followed by a Tukey's honestly significant different (HSD) post hoc test. In qRT-PCR experiments, monochromatic LED conditions (red or blue) were compared to white light using a two-sided Student's *t*-test. All measurements were plotted into graphs using GraphPad Prism 5 software. In the graphs, the colours of the dots and lines indicate white, red, and blue LED conditions. All photographs were taken with a Nikon D5300 camera and edited in ImageJ (Fiji). Schematic models were generated with BioRender software. Final figures were assembled using Microsoft PowerPoint.

Author contributions

KS and RO conceived and designed the experiments. KS performed the experiments and the statistical analysis. KS and RO analysed the results and wrote the manuscript.



Funding

This work was part of the research program “LED it be 50%” with project number 14212, which is partly financed by the Dutch Research Council (NWO).

Acknowledgements

We would like to thank Signify for providing the LED modules, and Cris Kuhlemeier for providing seeds of the tomato *pDR5::YFP* reporter. We acknowledge Fred Schenkel and Emiel Wiegiers for help with design and construction of the LED frame, and Peter Schellekens and Carlos Galvan-Ampudia for help with shoot apex dissection protocols.



References

- Abe, M., Kobayashi, Y., Yamamoto, S., Daimon, Y., Yamaguchi, A., Ikeda, Y., Ichinoki, H., Notaguchi, M., Goto, K., and Araki, T. (2005). FD, a bZIP protein mediating signals from the floral pathway integrator FT at the shoot apex. *Science* 309, 1052–1056.
- Ben-Gera, H., Shwartz, I., Shao, M. R., Shani, E., Estelle, M., and Ori, N. (2012). ENTIRE and GOBLET promote leaflet development in tomato by modulating auxin response. *Plant J.* 70, 903–915.
- Blázquez, M. A., and Weigel, D. (1999). Independent regulation of flowering by phytochrome B and gibberellins in Arabidopsis. *Plant Physiol.* 120, 1025–1032.
- Campoli, C., Drosse, B., Searle, I., Coupland, G., and Von Korff, M. (2012). Functional characterisation of HvCO1, the barley (*Hordeum vulgare*) flowering time ortholog of CONSTANS. *Plant J.* 69, 868–880.
- Cheng, X. F., and Wang, Z. Y. (2005). Overexpression of COL9, a CONSTANS-LIKE gene, delays flowering by reducing expression of CO and FT in *Arabidopsis thaliana*. *Plant J.* 43, 758–768.
- Cho, L. H., Yoon, J., and An, G. (2017). The control of flowering time by environmental factors. *Plant J.* 90, 708–719.
- Christians, M. J., Gingerich, D. J., Hua, Z., Lauer, T. D., and Vierstra, R. D. (2012). The light-response BTB1 and BTB2 proteins assemble nuclear ubiquitin ligases that modify phytochrome B and D signaling in Arabidopsis. *Plant Physiol.* 160, 118–134.
- Fornara, F., Panigrahi, K. C. S., Gissot, L., Sauerbrunn, N., Rühl, M., Jarillo, J. A., and Coupland, G. (2009). Arabidopsis DOF transcription factors act redundantly to reduce CONSTANS expression and are essential for a photoperiodic flowering response. *Dev. Cell* 17, 75–86.
- Franco-Zorrilla, J. M., Valli, A., Todesco, M., Mateos, I., Puga, M. I., Rubio-Somoza, I., Leyva, A., Weigel, D., García, A., and Paz-Ares, J. (2007). Target mimicry provides a new mechanism for regulation of microRNA activity. *Nat. Genet.* 39, 1033–1037.
- Huijser, P., and Schmid, M. (2011). The control of developmental phase transitions



Chapter 5: Light quality regulates flowering

in plants. *Development* 138, 4117–4129.

- Huq, E., Tepperman, J. M., and Quail, P. H.** (2000). GIGANTEA is a nuclear protein involved in phytochrome signaling in Arabidopsis. *Proc. Natl. Acad. Sci. U. S. A.* 97, 9789–9794.
- Jeong, S., and Clark, S. E.** (2005). Photoperiod regulates flower meristem development in *Arabidopsis thaliana*. *Genetics* 169, 907–915.
- Jung, J. H., Seo, Y. H., Pil, J. S., Reyes, J. L., Yun, J., Chua, N. H., and Park, C. M.** (2007). The GIGANTEA-regulated microRNA172 mediates photoperiodic flowering independent of CONSTANS in Arabidopsis. *Plant Cell* 19, 2736–2748.
- Karami, O., Rahimi, A., Khan, M., Bemer, M., Hazarika, R. R., Mak, P., Compier, M., van Noort, V., and Offringa, R.** (2020). A suppressor of axillary meristem maturation promotes longevity in flowering plants. *Nat. Plants* 6, 368–376.
- Koncz, C., Chua*, N.-H., Schell, J., and Rédei, G. P.** (1992). A heuristic glance at the past of Arabidopsis genetics. *Methods Arab. Res.* , 1–15.
- Lazaro, A., Mouriz, A., Piñeiro, M., and Jarillo, J. A.** (2015). Red light-mediated degradation of constans by the e3 ubiquitin ligase hos1 regulates photoperiodic flowering in Arabidopsis. *Plant Cell* 27, 2437–2454. .
- Lee, Z. H., Hirakawa, T., Yamaguchi, N., and Ito, T.** (2019). The roles of plant hormones and their interactions with regulatory genes in determining meristem activity. *Int. J. Mol. Sci.* 20, 4065.
- Li, J., Luan, Y., Zhai, J., Liu, P., and Xia, X.** (2013). Bioinformatic analysis of functional characteristics of miR172 family in tomato. *J. Northeast Agric. Univ.* 20, 19–27.
- Liu, L. J., Zhang, Y. C., Li, Q. H., Sang, Y., Mao, J., Lian, H. L., Wang, L., and Yang, H. Q.** (2008). COP1-mediated ubiquitination of CONSTANS is implicated in cryptochrome regulation of flowering in Arabidopsis. *Plant Cell* 20, 292–306.
- Livak, K. J., and Schmittgen, T. D.** (2001). Analysis of relative gene expression data using real-time quantitative PCR and the 2- $\Delta\Delta$ CT method. *Methods* 25,



402–408.

- Martin-Tryon, E. L., Kreps, J. A., and Harmer, S. L.** (2007). GIGANTEA acts in blue light signaling and has biochemically separable roles in circadian clock and flowering time regulation. *Plant Physiol.* 143, 473–486.
- Mayfield, J. D., Folta, K. M., Paul, A. L., and Ferl, R. J.** (2007). The 14-3-3 proteins μ and ν influence transition to flowering and early phytochrome response. *Plant Physiol.* 145, 1692–1702.
- McCloy, R. A., Rogers, S., Caldon, C. E., Lorca, T., Castro, A., and Burgess, A.** (2014). Partial inhibition of Cdk1 in G2 phase overrides the SAC and decouples mitotic events. *Cell Cycle* 13, 1400–1412.
- Monte, E., Alonso, J. M., Ecker, J. R., Zhang, Y., Li, X., Young, J., Austin-Phillips, S., and Quail, P. H.** (2003). Isolation and characterization of phyC mutants in Arabidopsis reveals complex crosstalk between phytochrome signaling pathways. *Plant Cell* 15, 1962–1980.
- Morrow, R. C.** (2008). LED lighting in horticulture. *HortScience* 43, 1947–1950.
- Ottenschläger, I., Wolff, P., Wolverton, C., Bhalerao, R. P., Sandberg, G., Ishikawa, H., Evans, M., and Palme, K.** (2003). Gravity-regulated differential auxin transport from columella to lateral root cap cells. *Proc. Natl. Acad. Sci. U. S. A.* 100, 2987–2991.
- Pratt, L. H., Cordonnier-Pratt, M. M., Hauser, B., and Caboche, M.** (1995). Tomato contains two differentially expressed genes encoding B-type phytochromes, neither of which can be considered an ortholog of Arabidopsis phytochrome B. *Planta* 197, 203–206.
- Rahimi, A., Karami, O., Balazadeh, S., and Offringa, R.** (2022). miR156-independent repression of the ageing pathway by longevity-promoting AHL proteins in Arabidopsis. *New Phytol.* 235, 2424–2438.
- Reed, J. W., Nagpal, P., Poole, D. S., Furuya, M., and Chory, J.** (1993). Mutations in the gene for the red/far-red light receptor phytochrome B alter cell elongation and physiological responses throughout Arabidopsis development. *Plant Cell* 5, 147–157.
- Robert, L. S., Robson, F., Sharpe, A., Lydiate, D., and Coupland, G.** (1998).



Chapter 5: Light quality regulates flowering

Conserved structure and function of the *Arabidopsis* flowering time gene *CONSTANS* in *Brassica napus*. *Plant Mol. Biol.* 37, 763–772.

Ruckle, M. E., DeMarco, S. M., and Larkin, R. M. (2007). Plastid signals remodel light signaling networks and are essential for efficient chloroplast biogenesis in *Arabidopsis*. *Plant Cell* 19, 3944–3960.

Salinas, M., Xing, S., Höhmann, S., Berndtgen, R., and Huijser, P. (2012). Genomic organization, phylogenetic comparison and differential expression of the SBP-box family of transcription factors in tomato. *Planta* 235, 1171–1184.

Samach, A., Onouchi, H., Gold, S. E., Ditta, G. S., Schwarz-Sommer, Z., Yanofsky, M. F., and Coupland, G. (2000). Distinct roles of *constans* target genes in reproductive development of *Arabidopsis*. *Science* 288, 1613–1616.

Sawa, M., Nusinow, D. A., Kay, S. A., and Imaizumi, T. (2007). FKF1 and GIGANTEA complex formation is required for day-length measurement in *Arabidopsis*. *Science* 318, 261–265.

Schindelin, J., Arganda-Carreras, I., Frise, E., Kaynig, V., Longair, M., Pietzsch, T., Preibish, S., Rueden, C., Saalfeld, S., Schmid, B., Tinevez, J. Y., White, D. J., Hartenstein, V., Eliceiri, K., Tomancak, P., and Cardona, A. (2012). Fiji: An open-source platform for biological-image analysis. *Nat. Methods* 9, 676–682.

Schwab, R., Palatnik, J. F., Riester, M., Schommer, C., Schmid, M., and Weigel, D. (2005). Specific effects of microRNAs on the plant transcriptome. *Dev. Cell* 8, 517–527.

Schwarz, S., Grande, A. V., Bujdoso, N., Saedler, H., and Huijser, P. (2008). The microRNA regulated SBP-box genes *SPL9* and *SPL15* control shoot maturation in *Arabidopsis*. *Plant Mol. Biol.* 67, 183–195.

SharathKumar, M., Heuvelink, E., and Marcelis, L. F. M. (2020). Vertical farming: moving from genetic to environmental modification. *Trends Plant Sci.* 25, 724–727.

Takase, T., Nishiyama, Y., Tanihigashi, H., Ogura, Y., Miyazaki, Y., Yamada, Y., and Kiyosue, T. (2011). *LOV KELCH PROTEIN2* and *ZEITLUPE* repress *Arabidopsis* photoperiodic flowering under non-inductive conditions, dependent



- on FLAVIN-BINDING KELCH REPEAT F - BOX1. *Plant J.* 67, 608–621.
- Telfer, A., Bollman, K. M., and Poethig, R. S.** (1997). Phase change and the regulation of trichome distribution in *Arabidopsis thaliana*. *Development* 124, 645–654.
- Teotia, S., and Tang, G.** (2015). To bloom or not to bloom: Role of microRNAs in plant flowering. *Mol. Plant* 8, 359–377.
- Thomas, B.** (2006). Light signals and flowering. *J. Exp. Bot.* 57, 3387–3393.
- Valverde, F., Mouradov, A., Soppe, W., Ravenscroft, D., Samach, A., and Coupland, G.** (2004). Photoreceptor regulation of CONSTANS protein in photoperiodic flowering. *Science* 303, 1003–1006.
- Wang, J. W., Schwab, R., Czech, B., Mica, E., and Weigel, D.** (2008). Dual effects of miR156-targeted SPL genes and CYP78A5/KLUH on plastochron length and organ size in *Arabidopsis thaliana*. *Plant Cell* 20, 1231–1243.
- Warnasooriya, S. N., Porter, K. J., and Montgomery, B. L.** (2011). Tissue- and isoform-specific phytochrome regulation of light-dependent anthocyanin accumulation in *Arabidopsis thaliana*. *Plant Signal. Behav.* 6, 624–631.
- Wigge, P. A., Kim, M. C., Jaeger, K. E., Busch, W., Schmid, M., Lohmann, J. U., and Weigel, D.** (2005). Integration of spatial and temporal information during floral induction in *Arabidopsis*. *Science* 309, 1056–1059.
- Wu, F., and Hanzawa, Y.** (2014). Photoperiodic control of flowering in plants. *Handbook of plant and crop physiology* 121–138.
- Wu, G., Park, M. Y., Conway, S. R., Wang, J. W., Weigel, D., and Poethig, R. S.** (2009). The sequential action of miR156 and miR172 regulates developmental timing in *Arabidopsis*. *Cell* 138, 750–759.
- Xie, Y., Liu, Y., Wang, H., Ma, X., Wang, B., Wu, G., and Wang, H.** (2017). Phytochrome-interacting factors directly suppress MIR156 expression to enhance shade-avoidance syndrome in *Arabidopsis*. *Nat. Commun.* 8, 348.
- Xie, Y., Zhou, Q., Zhao, Y., Li, Q., Liu, Y., Ma, M., Wang, B., Shen, R., Zheng, Z., and Wang, H.** (2020). FHY3 and FAR1 integrate light signals with the miR156-SPL module-mediated aging pathway to regulate *Arabidopsis*



Chapter 5: Light quality regulates flowering

flowering. *Mol. Plant* 13, 483–498.

- Yang, S., Weers, B. D., Morishige, D. T., and Mullet, J. E.** (2014). CONSTANS is a photoperiod regulated activator of flowering in sorghum. *BMC Plant Biol.* 14, 1–15.
- Yano, M., Katayose, Y., Ashikari, M., Yamanouchi, U., Monna, L., Fuse, T., Baba, T., Yamamoto, K., Umehara, Y., Nagamura, Y. and Sasaki, T.** (2000). Hd1, a major photoperiod sensitivity quantitative trait locus in rice, is closely related to the Arabidopsis flowering time gene CONSTANS. *Plant Cell* 12, 2473–2483.
- Yoshida, S., Mandel, T., and Kuhlemeier, C.** (2011). Stem cell activation by light guides plant organogenesis. *Genes Dev.* 25, 1439–1450.
- Zhang, X., Zou, Z., Zhang, J., Zhang, Y., Han, Q., Hu, T., Xu, X., Liu, H., Li, H., and Ye, Z.** (2011). Over-expression of sly-miR156a in tomato results in multiple vegetative and reproductive trait alterations and partial phenocopy of the sft mutant. *FEBS Lett.* 585, 435–439.
- Zheng, C., Ye, M., Sang, M., and Wu, R.** (2019). A regulatory network for mir156-spl module in *Arabidopsis thaliana*. *Int. J. Mol. Sci.* 20, 6166.



Supplementary Material (Tables S1-S3 and Figure S1-S3)

Table S1: Plant lines used in this study.

Arabidopsis, tomato, and lettuce seeds were obtained from Nottingham Arabidopsis Stock Centre (NASC), Tomato Genetics Resource Centre (TGRC), and HortiTops, respectively.

PLANT LINE	DESCRIPTION	SOURCE	REFERENCE
Columbia (Col-0)	Natural Arabidopsis ecotype	-	Koncz et al., 1992
Moneymaker (MM)	Standard non-hybrid tomato cultivar	TGRC	-
Meikoningin (MK)	Long-day lettuce cultivar	HortiTops	-
Gaardenier (GD)	Day-neutral lettuce cultivar	HortiTops	-
<i>phyA</i> (SALK_014575)	T-DNA insertion in At1g09570	NASC	Ruckle et al., 2007
<i>phyB</i> (SALK_022035)	T-DNA insertion in At2g18790	NASC	Mayfield et al., 2007
<i>phyC</i> (<i>phyC-3</i>)	3 kbp deletion in At5g35840	NASC	Monte et al., 2003
<i>phyD</i> (SALK_027956)	T-DNA insertion in At4g16250	NASC	Christians et al., 2012
<i>phyE</i> (SALK_092529)	T-DNA insertion in At4g18130	NASC	Warnasooriya et al., 2011
<i>ztl</i> (SALK_069091)	T-DNA insertion in At5g57360	NASC	Martin-Tryon et al., 2007
<i>fkf1</i> (SALK_059480)	T-DNA insertion in At1g68050	NASC	Cheng and Wang, 2005
<i>lkp2</i> (SALK_036083)	T-DNA insertion in At2g18915	NASC	Takase et al., 2011
<i>spl9 spl15</i>	Double mutant in At2g42200 and At3g57920	NASC	Schwarz et al., 2008
<i>p35S::miR156b</i>	Overexpression of <i>miR156</i> in Col-0	NASC	Schwab et al., 2005
<i>p35S::MIM156</i>	Overexpression of <i>miR156</i> target mimic in Col-0	NASC	Franco-Zorrilla et al., 2007
<i>pDR5::GFP</i>	Synthetic auxin-responsive reporter in Col-0	-	Ottenschläger et al., 2003



Chapter 5: Light quality regulates flowering

<i>pDR5::YFP</i>	Synthetic auxin-responsive reporter in tomato M82	Kuhlemeier	Ben-Gera et al., 2012
------------------	---------------------------------------------------	------------	-----------------------

Table S2: Primers used in this study.

PRIMER NAME	TARGET GENE	SEQUENCE 5' → 3'	EXPERIMENT
LB1 (SAIL T-DNA)	N/A	GCCTTTTCAGAA ATGGATAAATA	Genotyping
LBb1.3 (SALK T-DNA)	N/A	ATTTTGCCGATT TCGGAAC	Genotyping
<i>phyA</i> FW	At1g09570	CCAGTCAGCTCA GCAATTTTC	Genotyping
<i>phyA</i> RV	At1g09570	AATGCAAAACAT GCTAGGGTG	Genotyping
<i>phyB</i> FW	At2g18790	CATCATCAGCAT CATGTCACC	Genotyping
<i>phyB</i> RV	At2g18790	TTCACGAAGGCA AAAGAGTTG	Genotyping
<i>phyC</i> FW	At5g35840	ATGTCATCGAAC ACTTCACG	Genotyping
<i>phyC</i> RV	At5g35840	TCAAATCAAGGG AAATTCTG	Genotyping
<i>phyD</i> FW	At4g16250	AACCCGGTAGAA TCAGAATGG	Genotyping
<i>phyD</i> RV	At4g16250	ATCGGTTACAGT GAAAATGCG	Genotyping
<i>phyE</i> FW	At4g18130	AAAGAGGCGGT CTAGTTCAGC	Genotyping
<i>phyE</i> RV	At4g18130	TATCAGTGGTTA AACCCGTCG	Genotyping
<i>ztl</i> FW	At5g57360	GGACCGTTTGCT AAAAGAAGG	Genotyping
<i>ztl</i> RV	At5g57360	GTGTCACTTAGA AGAACGCCG	Genotyping
<i>fkf1</i> FW	At1g68050	GCATGGTCGAGT AACAAGGAG	Genotyping
<i>fkf1</i> RV	At1g68050	TGATGCAGAGTG	Genotyping



<i>lkp2</i> FW	At2g18915	TCCTGAGTG GGAGATCCATCT TTCCGAAAG	Genotyping
<i>lkp2</i> RV	At2g18915	CTCTTTTCTTCGC TCGATTCC	Genotyping
<i>spl9</i> FW	At2g42200	TGGTTCCTCCACT GAGTCATC	Genotyping
<i>spl9</i> RV	At2g42200	GCTCATTATGAC CAGCGAGTC	Genotyping
<i>spl15</i> FW	At3g57920	TGTTGGTGTCTG AAGTTGCTG	Genotyping
<i>spl15</i> RV	At3g57920	TCCACCGAGTCT TCTTCACTC	Genotyping
SnoR101 RV		AGCATCAGCAGA CCAGTAGTT	RT miRNA
miR156 FW-RT	At2g25095	GTCGTATCCAGTG CAGGGTCCGAGGT ATTCGCACTGGAT ACGACGTGCTCA	RT miRNA
miR172 FW-RT	At5g04275	GTCGTATCCAGTG CAGGGTCCGAGGT ATTCGCACTGGAT ACGACATGCAG	RT miRNA
PP2A-3 FW	At2g42500	ACGTGGCCAAAA TGATGCAA	qRT-PCR
PP2A-3 RV	At2g42500	TCATGTTCTCCAC AACCGCT	qRT-PCR
GIGANTEA FW	At1g22770	GGGTAAATATGC TGCTGGAGA	qRT-PCR
GIGANTEA RV	At1g22770	CAGTATGACACC AGCTCCATT	qRT-PCR
CONSTANS FW	At5g15840	CTACAACGACAA TGGTTCCATTAAC	qRT-PCR
CONSTANS RV	At5g15840	CAGGGTCAGGTT GTTGC	qRT-PCR
FT FW	At1g65480	CTGGAACAACCT TTGGCAAT	qRT-PCR
FT RV	At1g65480	TACACTGTTTGCC TGCCAAG	qRT-PCR
miR156-A FW	At2g25095	CTTCGTTCTCTAT GTCTCAATCTCTC	qRT-PCR
miR156-A RV	At2g25095	TGATTAAAGGCT	qRT-PCR



Chapter 5: Light quality regulates flowering

		AAAGGTCTCCTC	
miR172-B FW	At5g04275	TTTCTCAAGCTTTA GGTATTTGTAG	qRT-PCR
miR172-B RV	At5g04275	TCGGCGGATCCATG GAAGAAAGCTC	qRT-PCR
AHL15 FW	At3g55560	AAGAGCAGCCGCTT CAACTA	qRT-PCR
AHL15 RV	At3g55560	TGTTGAGCCATTTGA TGACC	qRT-PCR
SPL2 FW	At5g43270	TTTCCGATACCGAGC ACAATAG	qRT-PCR
SPL2 RV	At5g43270	TACGGGTTGGAGGTT GCTTGAGG	qRT-PCR
SPL3 FW	At2g33810	ATGAGTATGAGAAGA AGCAAAGCG	qRT-PCR
SPL3 RV	At2g33810	TCCACTACTACTTGTA GCTTTACCT	qRT-PCR
SPL4 FW	At1g53160	TCAAGGGTAGAGATG ACACTTCCTAT	qRT-PCR
SPL4 RV	At1g53160	TCTCCTTCGTGGCTCT GAACTTC	qRT-PCR
SPL5 FW	At3g15270	CGATAGGTGCACTGTT AATTTGACT	qRT-PCR
SPL5 RV	At3g15270	TCTGGTAGCTCATGAA ACCTGCTGCA	qRT-PCR
SPL6 FW	At1g69170	ACAGTGCAGCAGGTTT CATTTCCTC	qRT-PCR
SPL6 RV	At1g69170	CTCCAGAACTTGTTG CCTACTAC	qRT-PCR
SPL9 FW	At2g42200	AATTGGCGACTCAAAC TGTG	qRT-PCR
SPL9 RV	At2g42200	CTGAAGAAGCTCGCC ATGTA	qRT-PCR
SPL10 FW	At1g27370	CAGACAAAGGTGTGG GAGAATGCTC	qRT-PCR
SPL10 RV	At1g27370	TAGGGAAAGTGCCAA ATATTGGCG	qRT-PCR
SPL11 FW	At1g27360	AGTCCAAGTTTCAACT TCATGGCG	qRT-PCR
SPL11 RV	At1g27360	GAACAGAGTAGAGAA AATGGCTGC	qRT-PCR
SPL13 FW	At5g50570	GCTCGAGAACCGCAT	qRT-PCR



		CGTT	
SPL13 RV	At5g50570	CCCGTAAAAAAC TGTCTCAACTGCT	qRT-PCR
SPL15 FW	At3g57920	TGAATGTTTTATC ACATGGAAGCTC	qRT-PCR
SPL15 RV	At3g57920	TCATCGAGTCGAA ACCAGAAGATG	qRT-PCR
SOC1 FW	At3g57920	ATAGGAACATGCT CAATCGAGGAGCTG	qRT-PCR
SOC1 RV	At3g57920	TTTCTTGAAGAAC AAGGTAACCCAATG	qRT-PCR

Table S3: Standard errors and p-values.

In some figures, error bars and statistics were not included in the graphs for presentation purposes. These values are listed in the table below. Significance indicates whether or not red or blue LED conditions are significantly different from white LED conditions, based on a two-sided Student's *t*-test ($p < 0.05$). Abbreviations that are used: Standard error (SE), Zeitgeber time (ZT); not available (N/A); days after germination (DAG); and phytochrome B mutant (*phyB*).

FIGURE	DATA POINT	MEAN \pm SE	SIGNIFICANCE	P-VALUE
3B	ZT0-WHITE	0.138 \pm 0.025	N/A	N/A
3B	ZT3-WHITE	0.233 \pm 0.046	N/A	N/A
3B	ZT6-WHITE	0.408 \pm 0.030	N/A	N/A
3B	ZT9-WHITE	0.861 \pm 0.073	N/A	N/A
3B	ZT12-WHITE	0.557 \pm 0.031	N/A	N/A
3B	ZT15-WHITE	0.175 \pm 0.049	N/A	N/A
3B	ZT18-WHITE	0.235 \pm 0.026	N/A	N/A
3B	ZT21-WHITE	0.105 \pm 0.003	N/A	N/A
3B	ZT24-WHITE	0.102 \pm 0.009	N/A	N/A
3B	ZT0-RED	0.184 \pm 0.040	No	0.479
3B	ZT3-RED	0.249 \pm 0.046	No	0.849
3B	ZT6-RED	0.328 \pm 0.047	Yes	0.041
3B	ZT9-RED	0.531 \pm 0.072	Yes	0.006
3B	ZT12-RED	0.559 \pm 0.051	No	0.976
3B	ZT15-RED	0.274 \pm 0.015	No	0.191
3B	ZT18-RED	0.154 \pm 0.008	No	0.073



Chapter 5: Light quality regulates flowering

3B	ZT21-RED	0.157±0.018	No	0.086
3B	ZT24-RED	0.137±0.008	No	0.088
3B	ZT0-BLUE	0.208±0.030	No	0.222
3B	ZT3-BLUE	0.366±0.021	Yes	0.039
3B	ZT6-BLUE	0.923±0.073	Yes	0.00081
3B	ZT9-BLUE	1.446±0.181	Yes	0.00094
3B	ZT12-BLUE	0.719±0.028	Yes	0.034
3B	ZT15-BLUE	0.293±0.036	No	0.186
3B	ZT18-BLUE	0.175±0.022	No	0.228
3B	ZT21-BLUE	0.139±0.016	No	0.159
3B	ZT24-BLUE	0.165±0.009	No	0.172
3C	ZT0-WHITE	0.324±0.048	N/A	N/A
3C	ZT3-WHITE	0.189±0.036	N/A	N/A
3C	ZT6-WHITE	0.133±0.005	N/A	N/A
3C	ZT9-WHITE	0.209±0.031	N/A	N/A
3C	ZT12-WHITE	0.351±0.005	N/A	N/A
3C	ZT15-WHITE	0.279±0.050	N/A	N/A
3C	ZT18-WHITE	0.426±0.019	N/A	N/A
3C	ZT21-WHITE	0.301±0.005	N/A	N/A
3C	ZT24-WHITE	0.233±0.027	N/A	N/A
3C	ZT0-RED	0.392±0.055	No	0.491
3C	ZT3-RED	0.302±0.039	Yes	0.047
3C	ZT6-RED	0.286±0.050	Yes	0.008
3C	ZT9-RED	0.240±0.032	No	0.604
3C	ZT12-RED	0.299±0.012	Yes	0.039
3C	ZT15-RED	0.311±0.039	No	0.103
3C	ZT18-RED	0.359±0.040	Yes	0.013
3C	ZT21-RED	0.324±0.026	No	0.319
3C	ZT24-RED	0.261±0.007	No	0.154
3C	ZT0-BLUE	0.484±0.043	Yes	0.041
3C	ZT3-BLUE	0.354±0.047	Yes	0.022
3C	ZT6-BLUE	0.319±0.025	No	0.114
3C	ZT9-BLUE	0.279±0.011	No	0.159
3C	ZT12-BLUE	0.453±0.048	Yes	0.004
3C	ZT15-BLUE	0.358±0.033	Yes	0.034
3C	ZT18-BLUE	0.532±0.041	Yes	0.007
3C	ZT21-BLUE	0.426±0.016	Yes	0.009
3C	ZT24-BLUE	0.357±0.017	Yes	0.009
3D	ZT0-WHITE	0.053±0.011	N/A	N/A
3D	ZT3-WHITE	0.071±0.003	N/A	N/A
3D	ZT6-WHITE	0.063±0.007	N/A	N/A
3D	ZT9-WHITE	0.038±0.004	N/A	N/A



3D	ZT12-WHITE	0.081±0.008	N/A	N/A
3D	ZT15-WHITE	0.291±0.017	N/A	N/A
3D	ZT18-WHITE	0.115±0.014	N/A	N/A
3D	ZT21-WHITE	0.094±0.026	N/A	N/A
3D	ZT24-WHITE	0.054±0.007	N/A	N/A
3D	ZT0-RED	0.007±0.0002	Yes	0.025
3D	ZT3-RED	0.013±0.002	Yes	0.0002
3D	ZT6-RED	0.016±0.001	Yes	0.007
3D	ZT9-RED	0.012±0.002	Yes	0.007
3D	ZT12-RED	0.025±0.003	Yes	0.007
3D	ZT15-RED	0.028±0.002	Yes	0.002
3D	ZT18-RED	0.039±0.006	Yes	0.016
3D	ZT21-RED	0.032±0.0004	Yes	0.024
3D	ZT24-RED	0.008±0.002	Yes	0.007
3D	ZT0-BLUE	0.179±0.011	Yes	0.003
3D	ZT3-BLUE	0.401±0.048	Yes	0.005
3D	ZT6-BLUE	0.364±0.033	Yes	0.002
3D	ZT9-BLUE	0.229±0.014	Yes	0.039
3D	ZT12-BLUE	0.539±0.016	Yes	0.003
3D	ZT15-BLUE	0.798±0.026	Yes	0.001
3D	ZT18-BLUE	1.258±0.076	Yes	0.0003
3D	ZT21-BLUE	0.355±0.083	Yes	0.006
3D	ZT24-BLUE	0.079±0.011	No	0.193
5A	5 DAG-WHITE	0.277±0.012	N/A	N/A
5A	10 DAG-WHITE	0.248±0.029	N/A	N/A
5A	15 DAG-WHITE	0.223±0.0007	N/A	N/A
5A	5 DAG-RED	0.299±0.067	No	0.807
5A	10 DAG-RED	0.251±0.006	No	0.550
5A	15 DAG-RED	0.214±0.038	No	0.861
5A	5 DAG-BLUE	0.201±0.016	Yes	0.003
5A	10 DAG-BLUE	0.167±0.004	Yes	0.002
5A	15 DAG-BLUE	0.102±0.009	Yes	0.001
5B	5 DAG-WHITE	0.007±0.0004	N/A	N/A
5B	10 DAG-WHITE	0.014±0.0007	N/A	N/A
5B	15 DAG-WHITE	0.025±0.0007	N/A	N/A
5B	5 DAG-RED	0.007±0.0004	No	0.791
5B	10 DAG-RED	0.014±0.0008	No	0.326
5B	15 DAG-RED	0.021±0.001	No	0.530
5B	5 DAG-BLUE	0.038±0.008	Yes	0.0009
5B	10 DAG-BLUE	0.045±0.003	Yes	0.0008
5B	15 DAG-BLUE	0.057±0.004	Yes	0.0008
5C	5 DAG-WHITE	1.023±0.036	N/A	N/A



Chapter 5: Light quality regulates flowering

5C	10 DAG-WHITE	1.478±0.062	N/A	N/A
5C	15 DAG-WHITE	2.174±0.026	N/A	N/A
5C	5 DAG-RED	1.588±0.169	Yes	0.009
5C	10 DAG-RED	1.910±0.091	Yes	0.027
5C	15 DAG-RED	2.355±0.258	No	0.601
5C	5 DAG-BLUE	1.071±0.037	No	0.485
5C	10 DAG-BLUE	1.539±0.066	No	0.217
5C	15 DAG-BLUE	2.422±0.506	No	0.709
5D	5 DAG-WHITE	1.038±0.002	N/A	N/A
5D	10 DAG-WHITE	1.173±0.028	N/A	N/A
5D	15 DAG-WHITE	1.363±0.135	N/A	N/A
5D	5 DAG-RED	0.956±0.217	No	0.697
5D	10 DAG-RED	1.149±0.132	No	0.821
5D	15 DAG-RED	1.268±0.104	No	0.669
5D	5 DAG-BLUE	1.892±0.176	Yes	0.0009
5D	10 DAG-BLUE	2.314±0.095	Yes	0.0008
5D	15 DAG-BLUE	2.701±0.509	Yes	0.0009
5E	5 DAG-WHITE	0.104±0.008	N/A	N/A
5E	10 DAG-WHITE	0.154±0.007	N/A	N/A
5E	15 DAG-WHITE	0.249±0.016	N/A	N/A
5E	5 DAG-RED	0.110±0.031	No	0.884
5E	10 DAG-RED	0.148±0.018	No	0.912
5E	15 DAG-RED	0.191±0.016	No	0.101
5E	5 DAG-BLUE	0.149±0.007	Yes	0.024
5E	10 DAG-BLUE	0.397±0.022	Yes	0.0009
5E	15 DAG-BLUE	0.548±0.030	Yes	0.0007
5F	5 DAG-WHITE	0.311±0.041	N/A	N/A
5F	10 DAG-WHITE	0.751±0.033	N/A	N/A
5F	15 DAG-WHITE	0.795±0.043	N/A	N/A
5F	5 DAG-RED	0.329±0.087	No	0.889
5F	10 DAG-RED	0.481±0.033	Yes	0.007
5F	15 DAG-RED	0.528±0.027	Yes	0.013
5F	5 DAG-BLUE	0.469±0.048	Yes	0.041
5F	10 DAG-BLUE	1.057±0.018	Yes	0.003
5F	15 DAG-BLUE	0.966±0.084	Yes	0.031
5G	5 DAG-WHITE	0.254±0.021	N/A	N/A
5G	10 DAG-WHITE	0.548±0.017	N/A	N/A
5G	15 DAG-WHITE	0.785±0.004	N/A	N/A
5G	5 DAG-RED	0.214±0.038	No	0.499
5G	10 DAG-RED	0.457±0.052	No	0.628
5G	15 DAG-RED	0.631±0.051	No	0.561



5G	5 DAG-BLUE	0.534±0.064	Yes	0.024
5G	10 DAG-BLUE	1.375±0.074	Yes	0.0007
5G	15 DAG-BLUE	1.405±0.148	Yes	0.0008
5H	5 DAG-WHITE	0.436±0.006	N/A	N/A
5H	10 DAG-WHITE	0.548±0.046	N/A	N/A
5H	15 DAG-WHITE	1.402±0.060	N/A	N/A
5H	5 DAG-RED	0.546±0.078	No	0.317
5H	10 DAG-RED	0.518±0.006	No	0.628
5H	15 DAG-RED	1.585±0.159	No	0.431
5H	5 DAG-BLUE	0.506±0.055	No	0.357
5H	10 DAG-BLUE	0.357±0.031	No	0.217
5H	15 DAG-BLUE	1.184±0.046	No	0.079
5I	5 DAG-WHITE	0.066±0.007	N/A	N/A
5I	10 DAG-WHITE	0.076±0.002	N/A	N/A
5I	15 DAG-WHITE	0.097±0.004	N/A	N/A
5I	5 DAG-RED	0.069±0.015	No	0.873
5I	10 DAG-RED	0.089±0.011	No	0.572
5I	15 DAG-RED	0.093±0.006	No	0.512
5I	5 DAG-BLUE	0.152±0.009	Yes	0.0005
5I	10 DAG-BLUE	0.165±0.007	Yes	0.0008
5I	15 DAG-BLUE	0.183±0.013	Yes	0.0006
6A	10 DAG-WHITE	1.173±0.028	N/A	N/A
6A	15 DAG-WHITE	1.363±0.135	N/A	N/A
6A	20 DAG-WHITE	2.766±0.125	N/A	N/A
6A	25 DAG-WHITE	3.089±0.049	N/A	N/A
6A	10 DAG-RED	1.149±0.132	No	0.821
6A	15 DAG-RED	1.268±0.104	No	0.669
6A	20 DAG-RED	2.676±0.007	No	0.588
6A	25 DAG-RED	2.727±0.051	No	0.371
6A	10 DAG-BLUE	2.314±0.095	Yes	0.0008
6A	15 DAG-BLUE	2.701±0.509	Yes	0.0009
6A	20 DAG-BLUE	3.663±0.133	Yes	0.0009
6A	25 DAG-BLUE	1.968±0.021	Yes	0.0006
6B	10 DAG-WHITE	0.071±0.0004	N/A	N/A
6B	15 DAG-WHITE	0.231±0.002	N/A	N/A
6B	20 DAG-WHITE	0.847±0.047	N/A	N/A
6B	25 DAG-WHITE	0.869±0.028	N/A	N/A
6B	10 DAG-RED	0.085±0.005	No	0.672
6B	15 DAG-RED	0.182±0.038	No	0.353
6B	20 DAG-RED	0.626±0.068	No	0.095
6B	25 DAG-RED	0.847±0.048	No	0.749



Chapter 5: Light quality regulates flowering

6B	10 DAG-BLUE	0.219±0.004	Yes	0.021
6B	15 DAG-BLUE	0.404±0.026	Yes	0.017
6B	20 DAG-BLUE	1.996±0.036	Yes	0.0007
6B	25 DAG-BLUE	1.392±0.028	Yes	0.003
6C	10 DAG-WHITE	0.154±0.007	N/A	N/A
6C	15 DAG-WHITE	0.249±0.016	N/A	N/A
6C	20 DAG-WHITE	0.329±0.012	N/A	N/A
6C	25 DAG-WHITE	0.395±0.020	N/A	N/A
6C	10 DAG-RED	0.148±0.018	No	0.912
6C	15 DAG-RED	0.191±0.016	No	0.101
6C	20 DAG-RED	0.196±0.019	No	0.124
6C	25 DAG-RED	0.285±0.018	No	0.219
6C	10 DAG-BLUE	0.397±0.022	Yes	0.0009
6C	15 DAG-BLUE	0.548±0.030	Yes	0.0007
6C	20 DAG-BLUE	0.597±0.005	Yes	0.008
6C	25 DAG-BLUE	0.623±0.017	Yes	0.005
6D	10 DAG-WHITE	0.751±0.033	N/A	N/A
6D	15 DAG-WHITE	0.795±0.043	N/A	N/A
6D	20 DAG-WHITE	0.617±0.041	N/A	N/A
6D	25 DAG-WHITE	0.617±0.008	N/A	N/A
6D	10 DAG-RED	0.481±0.033	Yes	0.007
6D	15 DAG-RED	0.528±0.027	Yes	0.013
6D	20 DAG-RED	0.474±0.020	No	0.065
6D	25 DAG-RED	0.494±0.015	No	0.078
6D	10 DAG-BLUE	1.057±0.018	Yes	0.003
6D	15 DAG-BLUE	0.966±0.084	Yes	0.031
6D	20 DAG-BLUE	0.759±0.024	No	0.072
6D	25 DAG-BLUE	0.503±0.037	No	0.077
6E	10 DAG-WHITE	0.548±0.017	N/A	N/A
6E	15 DAG-WHITE	0.785±0.004	N/A	N/A
6E	20 DAG-WHITE	0.579±0.041	N/A	N/A
6E	25 DAG-WHITE	0.811±0.039	N/A	N/A
6E	10 DAG-RED	0.457±0.052	No	0.628
6E	15 DAG-RED	0.631±0.051	No	0.561
6E	20 DAG-RED	0.514±0.037	No	0.338
6E	25 DAG-RED	0.586±0.020	No	0.092
6E	10 DAG-BLUE	1.375±0.074	Yes	0.0007
6E	15 DAG-BLUE	1.405±0.148	Yes	0.0008
6E	20 DAG-BLUE	0.685±0.016	No	0.081
6E	25 DAG-BLUE	0.716±0.032	No	0.192
6F	10 DAG-WHITE	0.076±0.002	N/A	N/A



6F	15 DAG-WHITE	0.097±0.004	N/A	N/A
6F	20 DAG-WHITE	0.127±0.003	N/A	N/A
6F	25 DAG-WHITE	0.361±0.007	N/A	N/A
6F	10 DAG-RED	0.089±0.011	No	0.572
6F	15 DAG-RED	0.093±0.006	No	0.512
6F	20 DAG-RED	0.109±0.012	No	0.299
6F	25 DAG-RED	0.312±0.022	No	0.163
6F	10 DAG-BLUE	0.165±0.007	Yes	0.0008
6F	15 DAG-BLUE	0.183±0.013	Yes	0.0006
6F	20 DAG-BLUE	0.371±0.004	Yes	0.0004
6F	25 DAG-BLUE	0.601±0.003	Yes	0.0003
6G	5 DAG-WHITE	0.0005±0.0001	N/A	N/A
6G	10 DAG-WHITE	0.0024±0.0009	N/A	N/A
6G	15 DAG-WHITE	0.0260±0.008	N/A	N/A
6G	20 DAG-WHITE	0.6470±0.087	N/A	N/A
6G	25 DAG-WHITE	0.8650±0.167	N/A	N/A
6G	5 DAG-RED	0.0003±0.0001	No	0.388
6G	10 DAG-RED	0.0005±0.0002	No	0.071
6G	15 DAG-RED	0.0007±0.0002	Yes	0.008
6G	20 DAG-RED	0.0011±0.0003	Yes	0.0009
6G	25 DAG-RED	0.0021±0.0002	Yes	0.0006
6G	5 DAG-BLUE	0.0009±0.0001	No	0.094
6G	10 DAG-BLUE	0.0050±0.001	No	0.127
6G	15 DAG-BLUE	0.8950±0.086	Yes	0.0005
6G	20 DAG-BLUE	1.7390±0.288	Yes	0.0004
6G	25 DAG-BLUE	0.2290±0.059	Yes	0.007
6H	5 DAG-WHITE	0.076±0.008	N/A	N/A
6H	10 DAG-WHITE	0.199±0.011	N/A	N/A
6H	15 DAG-WHITE	0.503±0.093	N/A	N/A
6H	20 DAG-WHITE	1.176±0.275	N/A	N/A
6H	25 DAG-WHITE	2.095±0.522	N/A	N/A
6H	5 DAG-RED	0.059±0.009	No	0.783
6H	10 DAG-RED	0.151±0.029	No	0.668
6H	15 DAG-RED	0.176±0.044	Yes	0.03
6H	20 DAG-RED	0.433±0.092	Yes	0.02
6H	25 DAG-RED	0.617±0.113	Yes	0.007
6H	5 DAG-BLUE	0.072±0.007	No	0.924
6H	10 DAG-BLUE	0.253±0.029	No	0.645
6H	15 DAG-BLUE	1.430±0.466	Yes	0.006
6H	20 DAG-BLUE	4.320±0.942	Yes	0.0004
6H	25 DAG-BLUE	2.545±0.618	No	0.781
7B	10 DAG-BLUE	0.251±0.029	N/A	N/A



Chapter 5: Light quality regulates flowering

7B	15 DAG-BLUE	0.337±0.027	N/A	N/A
7B	20 DAG-BLUE	1.253±0.166	N/A	N/A
7B	25 DAG-BLUE	0.219±0.031	No	0.481
7B	<i>phyB</i> 10 DAG-RED	0.349±0.041	No	0.844
7B	<i>phyB</i> 15 DAG-RED	1.081±0.129	Yes	0.006
7B	<i>phyB</i> 5 DAG-BLUE	0.249±0.021	No	0.911
7B	<i>phyB</i> 10 DAG-BLUE	0.382±0.066	No	0.625
7B	<i>phyB</i> 15 DAG-BLUE	1.492±0.063	No	0.073
7C	<i>phyB</i> 5 DAG-WHITE	0.381±0.041	N/A	N/A
7C	<i>phyB</i> 10 DAG-WHITE	0.309±0.005	N/A	N/A
7C	<i>phyB</i> 15 DAG-WHITE	0.252±0.026	N/A	N/A
7C	<i>phyB</i> 5 DAG-RED	0.394±0.052	No	0.812
7C	<i>phyB</i> 10 DAG-RED	0.304±0.012	No	0.772
7C	<i>phyB</i> 15 DAG-RED	0.222±0.044	No	0.544
7C	<i>phyB</i> 5 DAG-BLUE	0.388±0.052	No	0.851
7C	<i>phyB</i> 10 DAG-BLUE	0.343±0.020	No	0.592
7C	<i>phyB</i> 15 DAG-BLUE	0.226±0.052	No	0.492
7D	<i>phyB</i> 5 DAG-WHITE	0.031±0.003	N/A	N/A
7D	<i>phyB</i> 10 DAG-WHITE	0.056±0.009	N/A	N/A
7D	<i>phyB</i> 15 DAG-WHITE	0.156±0.044	N/A	N/A
7D	<i>phyB</i> 5 DAG-RED	0.029±0.008	No	0.932
7D	<i>phyB</i> 10 DAG-RED	0.054±0.019	No	0.873



7D	<i>phyB</i> 15 DAG-RED	0.129±0.013	No	0.684
7D	<i>phyB</i> 5 DAG-BLUE	0.035±0.006	No	0.889
7D	<i>phyB</i> 10 DAG-BLUE	0.059±0.003	No	0.932
7D	<i>phyB</i> 15 DAG-BLUE	0.118±0.009	No	0.425
7E	<i>phyB</i> 5 DAG-WHITE	1.216±0.024	N/A	N/A
7E	<i>phyB</i> 10 DAG-WHITE	1.301±0.055	N/A	N/A
7E	<i>phyB</i> 15 DAG-WHITE	1.382±0.020	N/A	N/A
7E	<i>phyB</i> 5 DAG-RED	1.195±0.056	No	0.728
7E	<i>phyB</i> 10 DAG-RED	1.326±0.058	No	0.814
7E	<i>phyB</i> 15 DAG-RED	1.296±0.121	No	0.595
7E	<i>phyB</i> 5 DAG-BLUE	1.241±0.071	No	0.526
7E	<i>phyB</i> 10 DAG-BLUE	1.339±0.059	No	0.732
7E	<i>phyB</i> 15 DAG-BLUE	1.237±0.137	No	0.439
7F	<i>phyB</i> 5 DAG-WHITE	0.205±0.037	N/A	N/A
7F	<i>phyB</i> 10 DAG-WHITE	0.306±0.053	N/A	N/A
7F	<i>phyB</i> 15 DAG-WHITE	0.488±0.051	N/A	N/A
7F	<i>phyB</i> 5 DAG-RED	0.197±0.035	No	0.466
7F	<i>phyB</i> 10 DAG-RED	0.219±0.046	No	0.329
7F	<i>phyB</i> 15 DAG-RED	0.442±0.021	No	0.523
7F	<i>phyB</i> 5 DAG-BLUE	0.219±0.031	No	0.782
7F	<i>phyB</i> 10 DAG-BLUE	0.349±0.029	No	0.583



Chapter 5: Light quality regulates flowering

7F	<i>phyB</i> 15 DAG-BLUE	0.434±0.045	No	0.551
7G	<i>phyB</i> 5 DAG-WHITE	0.199±0.062	N/A	N/A
7G	<i>phyB</i> 10 DAG-WHITE	0.314±0.031	N/A	N/A
7G	<i>phyB</i> 15 DAG-WHITE	0.326±0.051	N/A	N/A
7G	<i>phyB</i> 5 DAG-RED	0.128±0.037	No	0.417
7G	<i>phyB</i> 10 DAG-RED	0.203±0.024	Yes	0.007
7G	<i>phyB</i> 15 DAG-RED	0.212±0.062	Yes	0.006
7G	<i>phyB</i> 5 DAG-BLUE	0.187±0.018	No	0.622
7G	<i>phyB</i> 10 DAG-BLUE	0.372±0.029	No	0.185
7G	<i>phyB</i> 15 DAG-BLUE	0.387±0.023	No	0.172
7H	<i>phyB</i> 5 DAG-WHITE	0.247±0.044	N/A	N/A
7H	<i>phyB</i> 10 DAG-WHITE	0.462±0.014	N/A	N/A
7H	<i>phyB</i> 15 DAG-WHITE	0.681±0.145	N/A	N/A
7H	<i>phyB</i> 5 DAG-RED	0.223±0.066	No	0.483
7H	<i>phyB</i> 10 DAG-RED	0.398±0.039	No	0.273
7H	<i>phyB</i> 15 DAG-RED	0.679±0.072	No	0.993
7H	<i>phyB</i> 5 DAG-BLUE	0.239±0.051	No	0.728
7H	<i>phyB</i> 10 DAG-BLUE	0.442±0.033	No	0.681
7H	<i>phyB</i> 15 DAG-BLUE	0.673±0.168	No	0.978
7I	<i>phyB</i> 5 DAG-WHITE	0.092±0.005	N/A	N/A
7I	<i>phyB</i> 10 DAG-WHITE	0.148±0.007	N/A	N/A



7I	<i>phyB</i> 15 DAG-WHITE	0.217±0.069	N/A	N/A
7I	<i>phyB</i> 5 DAG-RED	0.087±0.004	No	0.726
7I	<i>phyB</i> 10 DAG-RED	0.118±0.007	No	0.087
7I	<i>phyB</i> 15 DAG-RED	0.208±0.029	No	0.928
7I	<i>phyB</i> 5 DAG-BLUE	0.095±0.005	No	0.891
7I	<i>phyB</i> 10 DAG-BLUE	0.155±0.020	No	0.805
7I	<i>phyB</i> 15 DAG-BLUE	0.208±0.015	No	0.923
S3A	10 DAG-WHITE	0.181±0.011	N/A	N/A
S3A	15 DAG-WHITE	0.236±0.016	N/A	N/A
S3A	20 DAG-WHITE	0.530±0.026	N/A	N/A
S3A	25 DAG-WHITE	1.052±0.041	N/A	N/A
S3A	10 DAG-RED	0.162±0.022	No	0.472
S3A	15 DAG-RED	0.183±0.020	No	0.178
S3A	20 DAG-RED	0.538±0.083	No	0.646
S3A	25 DAG-RED	0.726±0.037	No	0.102
S3A	10 DAG-BLUE	0.176±0.019	No	0.872
S3A	15 DAG-BLUE	0.244±0.031	No	0.858
S3A	20 DAG-BLUE	0.563±0.021	No	0.246
S3A	25 DAG-BLUE	1.431±0.019	No	0.192
S3B	10 DAG-WHITE	3.9E-05±9.3E-06	N/A	N/A
S3B	15 DAG-WHITE	0.0005±4.5E-05	N/A	N/A
S3B	20 DAG-WHITE	0.0001±9.4E-06	N/A	N/A
S3B	25 DAG-WHITE	0.0001±3.8E-06	N/A	N/A
S3B	10 DAG-RED	2.7E-05±1.1E-04	No	0.189
S3B	15 DAG-RED	0.0004±3.9E-05	No	0.377
S3B	20 DAG-RED	8.8E-05±1.5E-05	No	0.093
S3B	25 DAG-RED	0.0003±3.6E-05	No	0.096
S3B	10 DAG-BLUE	7.1E-05±7.3E-06	Yes	0.043
S3B	15 DAG-BLUE	0.001±0.0002	Yes	0.031
S3B	20 DAG-BLUE	0.0005±4.2E-05	Yes	0.041



Chapter 5: Light quality regulates flowering

S3B	25 DAG-BLUE	6.2E-05±2.6E-06	Yes	0.023
S3C	10 DAG-WHITE	0.314±0.013	N/A	N/A
S3C	15 DAG-WHITE	0.256±0.019	N/A	N/A
S3C	20 DAG-WHITE	0.242±0.017	N/A	N/A
S3C	25 DAG-WHITE	0.361±0.008	N/A	N/A
S3C	10 DAG-RED	0.384±0.009	No	0.584
S3C	15 DAG-RED	0.191±0.008	No	0.178
S3C	20 DAG-RED	0.211±0.010	No	0.279
S3C	25 DAG-RED	0.341±0.012	No	0.335
S3C	10 DAG-BLUE	0.314±0.067	No	0.913
S3C	15 DAG-BLUE	0.183±0.010	No	0.052
S3C	20 DAG-BLUE	0.225±0.014	No	0.569
S3C	25 DAG-BLUE	0.253±0.012	No	0.089
S3D	10 DAG-WHITE	0.548±0.046	N/A	N/A
S3D	15 DAG-WHITE	1.402±0.060	N/A	N/A
S3D	20 DAG-WHITE	1.207±0.051	N/A	N/A
S3D	25 DAG-WHITE	1.141±0.038	N/A	N/A
S3D	10 DAG-RED	0.518±0.006	No	0.628
S3D	15 DAG-RED	1.585±0.159	No	0.431
S3D	20 DAG-RED	1.263±0.097	No	0.695
S3D	25 DAG-RED	0.938±0.053	No	0.165
S3D	10 DAG-BLUE	0.357±0.011	No	0.172
S3D	15 DAG-BLUE	1.184±0.046	No	0.102
S3D	20 DAG-BLUE	0.876±0.044	No	0.118
S3D	25 DAG-BLUE	0.972±0.029	No	0.129

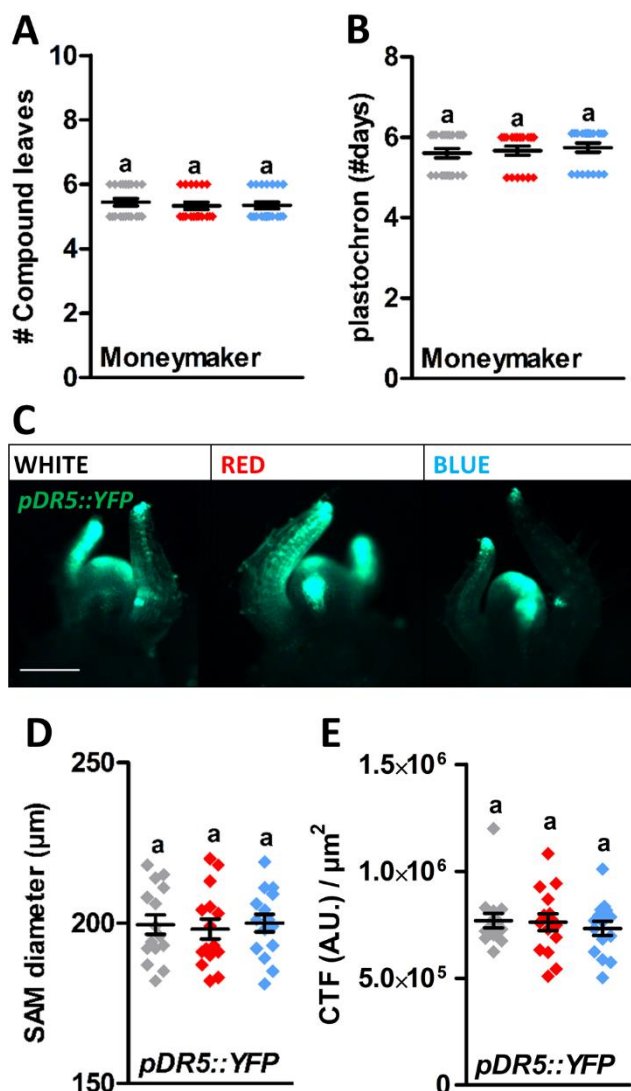


Figure S1: Tomato shoot development is indifferent to red and blue light.

A. Number of compound leaves of tomato cultivar Moneymaker (MM) plants grown in white, red, or blue LED conditions until the floral transition. **B.** Plastochron length (in number of days) of MM plants grown in the different LED conditions. **C.** Stereo-fluorescence microscopy images of representative shoot apices of tomato *pDR5::YFP* plants grown in the different LED conditions. **D.** SAM diameter (in μm) of tomato *pDR5::YFP* plants grown in the different LED conditions. **E.** Corrected Total Fluorescence (CTF) of the *pDR5::YFP* signal in Arbitrary Units (A.U.) in shoot apices of tomato plants grown in the different LED conditions.

Graph colours represent white, red, or blue LED conditions in **A**, **B**, **D** and **E**. Scale bars indicate 100 μm in **C**. LED conditions were compared using a one-way ANOVA followed by a Tukey's test (different letters indicate statistically significant differences, $p < 0.05$) in **A**, **B**, **D** and **E**. Error bars represent standard error from mean in **A**, **B**, **D** and **E**. Similar results were obtained in two independent experiments.

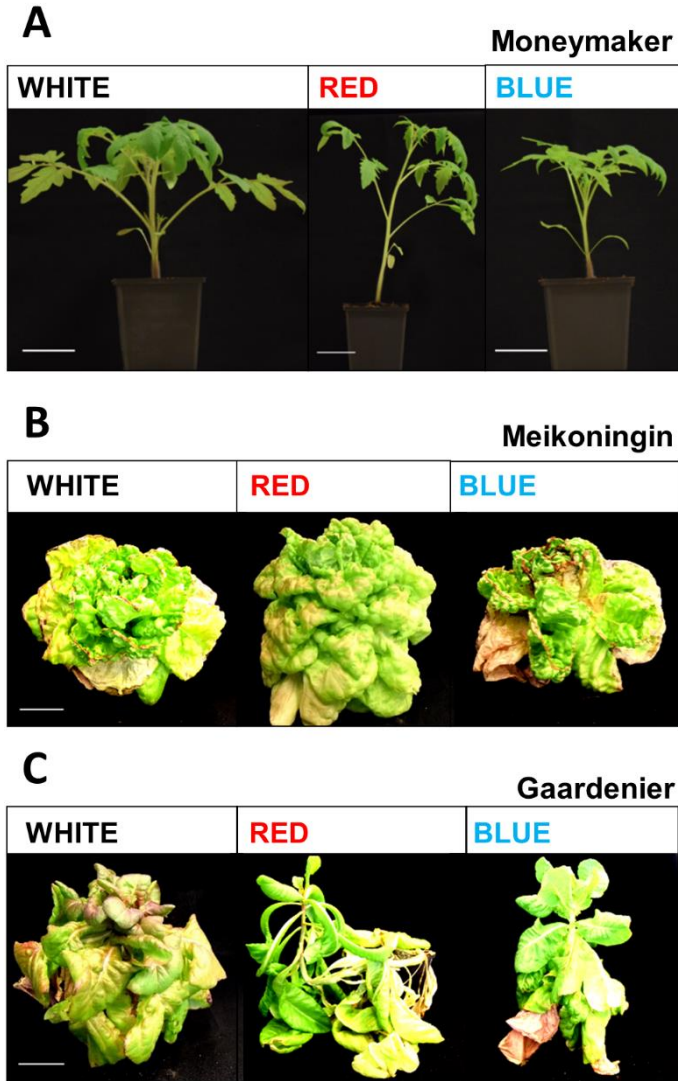


Figure S2: Phenotypes of tomato and lettuce plants grown in the LED conditions.

Representative tomato and lettuce plants that were grown in white, red, or blue LED conditions until the floral transition. **A.** 30-day-old tomato plants of the day-neutral cultivar Moneymaker. **B.** 12-weeks-old lettuce plants of the long-day variety Meikoningin. **C.** 12-weeks-old lettuce plants of the day-neutral variety Gaardenier. Scale bars indicate 5 cm in **A** and 10 cm in **B-C**. Similar results were obtained in either two (lettuce) or three (tomato) independent experiments.

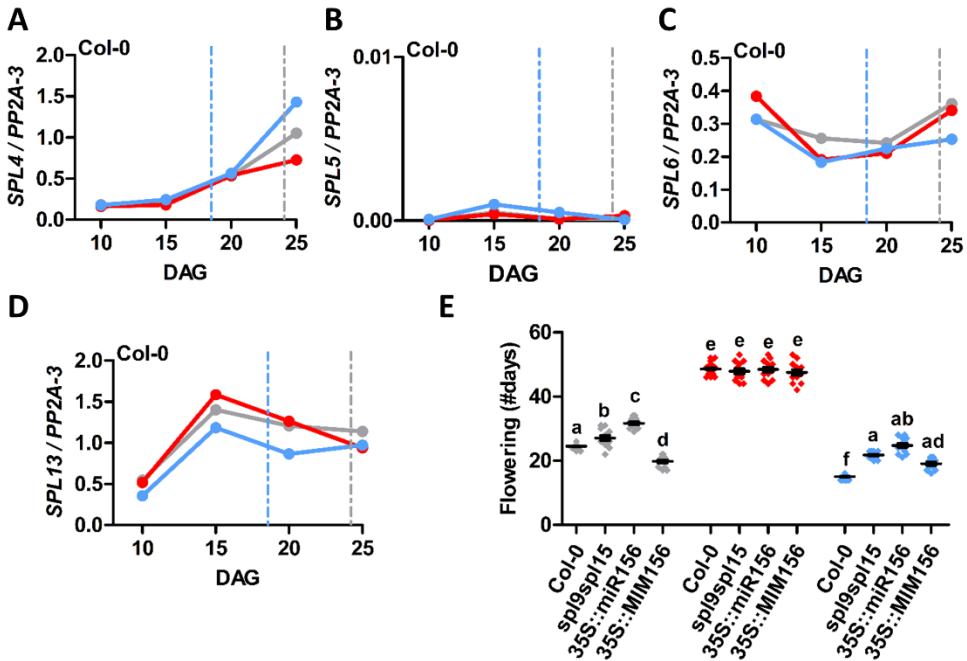


Figure S3: Early flowering in the absence of red light results from accelerated ageing.

A-D. Quantitative RT-PCR analysis of genes involved in the age pathway. Analysis was performed on Arabidopsis Columbia (Col-0) plants that were grown in white, red, or blue LED conditions at 10, 15, 20, and 25 days after germination (DAG). Relative expression levels of *SPL4* (**A**), *SPL5* (**B**), *SPL6* (**C**), and *SPL13* (**D**). **E.** Flowering time of Arabidopsis Columbia (Col-0), *p35S::miR156b*, *p35S::MIM156*, and *spl9 spl15* double mutant plants grown in the different LED conditions. Graph colours represent the different LED conditions. Monochromatic LED conditions (red or blue) were compared to white (control) using a two-sided Student's *t*-test (asterisks indicate significant differences at a specific time point (**p*<0.05)) in **A-D**. In **E**, LED conditions and wild types or mutants were compared using a one-way ANOVA followed by a Tukey's test (letters **a**, **b**, **c**, **d**, **e**, and **f** indicate statistically significant differences, *p*<0.05). Error bars represent standard error from mean in **E** (*n*=30), standard errors and *p*-values for **A-D** are listed in **Table S3**. Similar results were obtained in three (**A-D**) or two (**E**) independent experiments.

